Review | Received 7 October 2024; Accepted 23 December 2024; Published 21 January 2025
https://doi.org/10.55092/aimat20250004

Integrating AI and material science: MXene synthesis, preparation, and applications

Kexin Lv [1], Hengcheng Wan [2,3,*], Chenchen Qi [1], Wenwei Wang [1], Xiang Liu [2], Lei Zhang [2], Hongsen Wei [2], Hongjie Zhu [2], Yumo Wang [2], Juhong Yu [1,*] and Shiyu Du [1,4,5,*]

[1] School of Materials Science and Engineering, China University of Petroleum (East China), Qingdao, China
[2] Civil Aircraft Fire Science and Safety Engineering Key Laboratory of Sichuan Province, Civil Aviation Flight University of China, Guanghan, Sichuan, China
[3] College of Smart Energy Shanghai Jiao Tong University, Shanghai, China
[4] Zhejiang Key Laboratory of Data-Driven High-Safety Energy Materials and Applications, Ningbo Institute of Materials Technology and Engineering, Chinese Academy of Sciences, Ningbo 315201, P. R. China
[5] Milky-Way Sustainable Energy Ltd, Zhuhai, China

* Correspondence authors; E-mails: Wan_hengcheng@sjtu.edu.cn (H.W.); 20230031@upc.edu.cn (J.Y.); dushiyu@nimte.ac.cn (S.D.).

Highlights:

- Adjusting MXene interlayer spacing enhances ionic conductivity and stability in membranes.
- AI predicts MXene preparation and enables applications in AI devices like memristors.
- Regulated MXene membranes show promise in energy storage, hydrogen production, and AI.

Abstract: Recent research on two-dimensional anion exchange membranes has highlighted the potential of MXene-based anion exchange membranes in advanced applications. This review provides a comprehensive summary of the preparation strategies for high-quality MXene materials, including methods such as hydrofluoric acid (HF) etching, electrochemical processes, hydrothermal synthesis, and artificial intelligence (AI)-assisted approaches. Various film-forming techniques, such as vacuum filtration, casting, electrospinning, and AI-driven neural network optimization, are also discussed for their role in producing uniform and stable MXene membranes. A detailed examination of interlayer spacing regulation reveals its critical influence on ion exchange membrane performance, particularly with regard to ion transport mechanisms, rates, pathways, selective permeability, and membrane stability. AI has emerged as a transformative tool in this domain, significantly enhancing material discovery and optimization processes by improving synthesis efficiency and tailoring properties for specific applications. The review further explores advanced strategies for interlayer spacing regulation,

including surface functionalization, intercalation chemistry, composite formation with nanomaterials and polymers, and predictive modeling using neural networks. Beyond conventional applications in energy storage and catalysis, MXene materials demonstrate exceptional promise in AI-related fields due to their outstanding electrical conductivity, tunable surface chemistry, and mechanical flexibility. These properties position MXenes as key enablers for next-generation AI hardware systems, such as neuromorphic computing, intelligent sensing, and data storage. This work underscores the importance of integrating MXene research with AI to drive future advancements in both materials science and emerging technologies.

Keywords: MXene; artificial intelligence; electrolysis; hydrogen production; anion exchange membrane

1. Introduction

As the energy crisis intensifies and environmental pollution worsens, increasing attention has been directed towards the development of renewable energy sources, including solar power and hydrogen energy [1,2]. The increasingly widespread application of hydrogen energy has also led to a shortage of hydrogen gas supply [3]. In order to efficiently produce hydrogen, excellent hydrogen production methods have become one of the research hotspots [4]. Water electrolysis is widely recognized as a key technology for hydrogen production. Currently, four primary methods are employed for this purpose, namely: alkaline electrolyzer (AE) [5], proton exchange membrane electrolyzer (PEME) [6], anion exchange membrane electrolyzer (AEME) [7], and solid oxide electrolyzer (SOE) [8].

AEME is a green and sustainable hydrogen production technology [9], which has significant characteristics such as environmental friendliness, safety and reliability [10]. A key element of Anion Exchange Membrane Electrolyzers (AEMEs) is the anion exchange membrane (AEM) [11], which serves a vital function within the electrolyzer system. AEMs can quickly transfer hydroxide ions within the electrolyzer to improve electrolysis efficiency [12]. At the same time, AEMs also have the function of isolating the cathode and anode, preventing the generated gases (such as hydrogen and oxygen) from mixing, thereby ensuring product purity and system safety [13].

The selection and optimization of AEM materials have a perceptible effect on the efficiency of the electrolyzer [14]. In actual AEME, the required hydroxide ion conductive membrane should meet the following requirements [15]: high hydroxide conductivity, high alkali resistance, strong mechanical stability, low hydrogen permeability, and low cost for large-scale preparation (Figure 1). Modern technology enhances the stability and conductivity of the membrane by introducing different chemical modifications [16] and structural designs [17], so that it can still maintain good performance under alkaline and high current conditions. To enhance the ion transport efficiency of the anion exchange membrane, adjustments and optimizations are often implemented to improve its performance, the use of two-dimensional inorganic materials with layered structures to construct ion transfer channels on the film [18] is one of the effective ways to accelerate ion transfer. At present, the widely used inorganic two-dimensional materials are GO [19], LDH [20], and MXene [21] (Figure 1).

In 2011, Gogotsi and his team introduced a novel category of two-dimensional (2D) materials known as MXenes [22]. It is usually expressed as: $M_{n+1}X_nT_x$, where M is a transition metal, X is carbon (C) or nitrogen (N), n is an integer, typically 1 or 2, and T_x denotes surface functional groups on MXene (such as -OH, -O, or -F), which are introduced during the etching process. As a popular material with van der Waals heterostructure, MXene has shown great potential in ion transport, electron conduction,

particle screening, *etc*., so it can be applied to anion exchange membranes. At present, MXene has been applied in many fields, as shown in Figure 2: batteries [23], supercapacitors [24], photocatalysts [25], catalysts [26], sensors [27], adsorbents [28], transparent conductive films [29], electromagnetic interference shielding [30] and flexible high-strength composite materials [31].

The interlayer spacing of 2D van der Waals structure materials has a crucial influence on the performance of 2D material-based AEMs [32]. The regulation of interlayer spacing can significantly change the ion conduction path and conduction rate of AEMs. Properly increasing the interlayer spacing can increase the diffusion channels for anions (such as hydroxide ions, OH^-), reduce the resistance to ion transport, and thus improve the ion conductivity. Nonetheless, overly large interlayer spacing can result in reduced mechanical strength and potential structural instability of the membrane, thereby affecting the overall performance and service life of the membrane. In addition, the regulation of interlayer spacing also affects the selectivity of the membrane [33], efficiently conducting the target ions while rejecting other ions and molecules, thereby improving the selectivity and efficiency of the membrane.

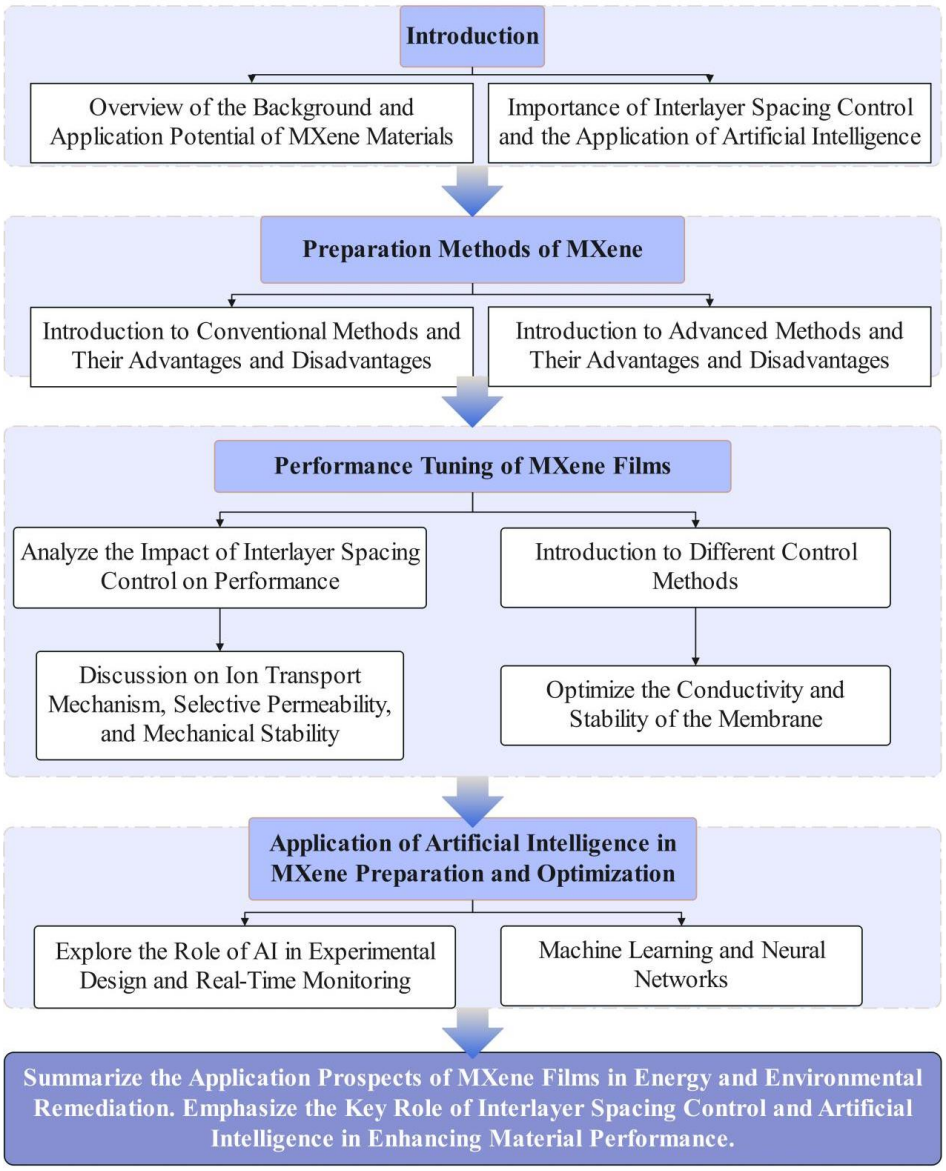

Figure 1. Logical framework diagram.

Similar to other 2D van der Waals structure materials, MXene has excellent hydrophilicity. When used in a water-rich environment, there are only some weak intermolecular forces between its layers, so it is very easy for the interlayers to be filled with water molecules and form hydrogen bonds [34]. This situation causes the interlayer spacing of MXene to expand in a disordered and chaotic manner, and the molecular permselectivity decreases, and the mechanical properties are greatly reduced.

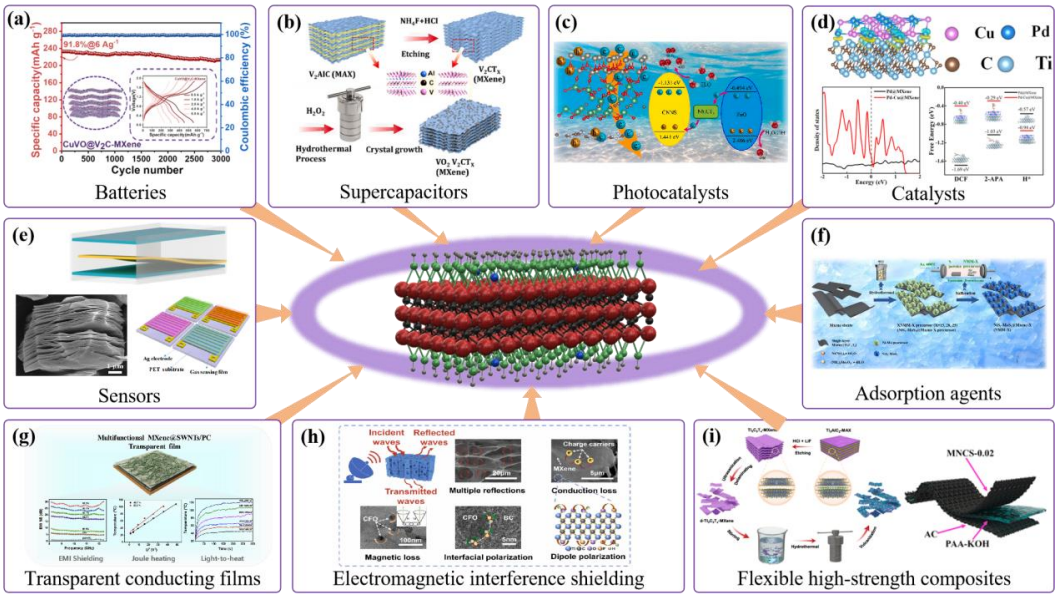

Figure 2. Applications of MXene. **(a)** Batteries. Reprinted with permission [23]. Copyright 2024 Elsevier. **(b)** Supercapacitors. Reprinted with permission [24]. Copyright 2024 Elsevier. **(c)** Photocatalysts. Reprinted with permission [25]. Copyright 2024 Elsevier. **(d)** Catalysts. Reprinted with permission [26]. Copyright 2024 Elsevier. **(e)** Sensors. Reprinted with permission [27]. Copyright 2024 Elsevier. **(f)** Adsorbents. Reprinted with permission [28]. Copyright 2024 Elsevier. **(g)** Transparent conductive films. Reprinted with permission [29]. Copyright 2024 Elsevier. **(h)** Electromagnetic interference shielding. Reprinted with permission [30]. Copyright 2024 Elsevier. **(i)** Flexible high-strength composites. Reprinted with permission [31]. Copyright 2024 Elsevier.

In recent years, the application of artificial intelligence in materials science has developed rapidly, greatly promoting the design and optimization of new materials [35]. Particularly in MXene research, AI enables optimized design and predictive capabilities. Successful applications of AI in MXene research include stability prediction [36], mechanical property optimization [37], cytotoxicity assessment [38], and bandgap prediction [39]. At the same time, machine learning, neural networks, and other methods have gradually been applied by researchers as auxiliary tools in the preparation and transformation of MXene [40]. First, AI technology can optimize the preparation process of MXene through big data and machine learning algorithms. For example, by analyzing extensive experimental data, AI can determine the optimal synthesis conditions and parameters, thereby enhancing the material's performance and improving the efficiency of its preparation process [41]. Secondly, AI can also be used to monitor and control the preparation process of MXene membranes in real time. By integrating sensors and intelligent control systems, AI can dynamically adjust the preparation parameters to ensure the quality and consistency of the membrane [42]. In addition to the preparation of MXene with the

assistance of artificial intelligence, MXene materials also have broad application prospects [43]. For example, applying MXene to gas monitoring, humidity monitoring, and biological detection sensors can improve the sensitivity and response speed of sensors [44]; applying MXene to neuromorphic computing and storage devices, as a synaptic material in artificial neural networks, can achieve brain-like computing and improve data storage capacity and read and write speeds [45]; or applying MXene to flexible electronic devices to prepare wearable smart devices to achieve real-time monitoring and intelligent feedback [46].

This paper aims to review and analyze the advancements in research on the regulation of MXene membrane interlayer spacing, as well as the performance optimization and applications achieved through artificial intelligence assistance. By systematically combing the existing literature, the traditional methods of preparing MXene materials and AI-assisted preparation methods are summarized, and on this basis, the traditional preparation methods and AI-assisted preparation methods of MXene-based exchange membranes are further summarized. Then, this paper discusses the principles, advantages, and limitations of various methods for regulating MXene interlayer spacing. It also reviews the utilization of AI technology in this field and examines how changes in interlayer spacing affect key membrane properties, including anion conductivity, selective permeability, and mechanical stability. Additionally, specific application cases are analyzed to assess the effectiveness and potential of these regulation techniques in real-world applications, providing a scientific foundation and reference for future research and engineering practices.

2. Synthesis strategy of MXene

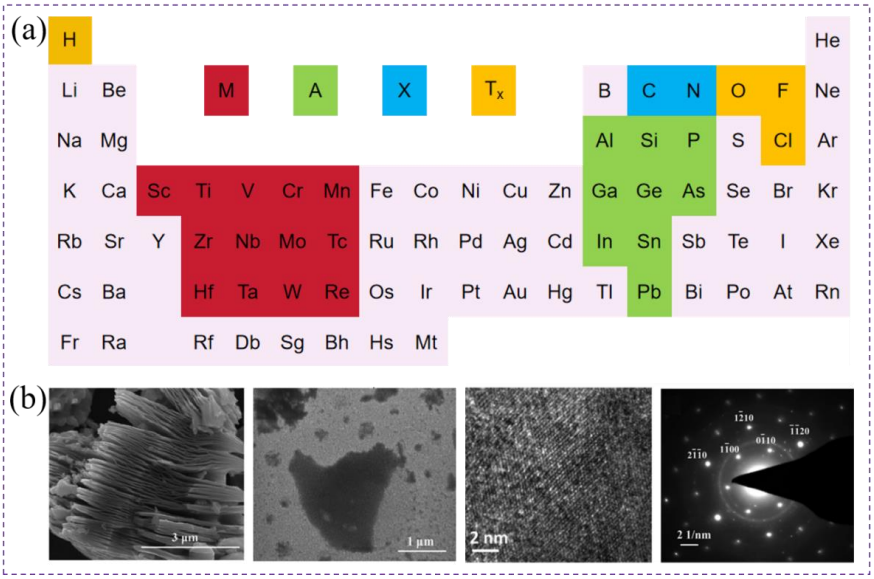

Figure 3. (a) Elemental constituents of MAX and MXenes. **(b)** The SEM, HRTEM, and selected area electron diffraction (SAED) analyses of Ti_3AlC_2 MAX phase powder following aluminum removal with HF are presented. Reprinted with permission [47]. Copyright 2017 ACS Publications.

Since the microstructure of the material obtained after etching the A layer in the MAX phase resembles the lamellar structure of graphene, it is referred to as MXene. The MAX phase materials are represented by the molecular formula $M_{n+1}AX_n$, where M denotes an early transition metal, A represents an element from groups 13 or 14, and X corresponds to either carbon (C) or nitrogen (N) [48]. As shown

in Figure 3(a), the MAX phase material has a layered hexagonal structure (space group P63/mmc), and each unit contains two formula units, in which the close-packed M layers and A group element layers are arranged in a staggered configuration, with X atoms occupying the octahedral sites between the M layers and the A group element layers in the MAX phase structure. During the etching of the A layer elements in the MAX phase material, the strong covalent and ionic bonds between the M atoms and the X atoms are retained, while the weaker MA-type metal bonds are destroyed, forming a two-dimensional layered symmetrical hexagonal structure [47]. The chemical formula of MXene is typically written as $M_{n+1}X_nT_x$, where T denotes surface termination groups, such as -OH, -O, or -F, which are introduced during the etching process [49,50].

MXenes can be synthesized using a range of etching techniques, such as hydrofluoric acid methods (including direct HF etching and *in situ* HF etching), electrochemical approaches, hydrothermal methods, molten salt substitution, algae-based extraction, photolithography, scalable production techniques, as well as iodine-assisted processes and ion-induced gelation, among others [51]. This section first explains several traditional chemical preparation methods: hydrofluoric (HF) acid preparation, electrochemical etching, and hydrothermal synthesis, and then introduces the method of preparing MXene with the assistance of artificial intelligence.

2.1. HF etching

In 2011, Gogotsi *et al.* prepared MXene for the first time using hydrofluoric acid etching [22]. Therefore, hydrofluoric acid etching is one of the most widely used techniques for MXene preparation. This method can be categorized into two main types: direct hydrofluoric acid etching and *in situ* hydrofluoric acid etching [52,53]. Direct hydrofluoric acid etching involves the removal of the A-phase from the MAX phase structure using hydrofluoric acid, converting the dense MAX phase into a multi-layer accordion-shaped MXene, and the surface of the remaining MX layers develops functional groups such as -OH, -F, -O. The reaction can be represented as follow:

$$2Ti_3AlC_2 + 6HF = 3H_2\uparrow + 2Ti_3C_2 + 2AlF_3 \quad (1)$$

$$2Ti_3C_2 + 2HF = Ti_3C_2(F)_2 + H_2\uparrow \quad (2)$$

$$Ti_3C_2 + 2H_2O = Ti_3C_2(OH)_2 + 2H_2\uparrow \quad (3)$$

$$Ti_3C_2 + 2H_2O = Ti_3C_2(O)_2 + 2H_2\uparrow \quad (4)$$

Ghidiu *et al.* [53] introduced an *in situ* hydrofluoric acid etching approach, where various etchants are utilized to produce hydrofluoric acid directly within the reaction environment. This *in situ* generated hydrofluoric acid is then used to remove aluminum (Al) from Ti_3AlT_x [54,55]. The MXene generated after etching has surface functional groups such as -O, -OH, and -F [56]. Since the MXene generated by this method is a paste and has a clay-like appearance, this *in situ* hydrofluoric acid etching method is also called the “clay method” [57]. The chemical reaction formula during the etching process can be expressed as follows:

$$Ti_3AlC_2 + 3HCl + 3LiF = Ti_3C_2 + 3LiCl + AlF_3 + 1.5H_2\uparrow \quad (5)$$

$$Ti_3C_2 + 2HF = Ti_3C_2(F)_2 + H_2\uparrow \quad (6)$$

$$Ti_3C_2 + 2HCl = Ti_3C_2(Cl)_2 + H_2\uparrow \quad (7)$$

$$Ti_3C_2 + 2H_2O = Ti_3C_2(OH)_2 + H_2\uparrow \quad (8)$$

$$Ti_3C_2 + 2H_2O = Ti_3C_2(O)_2 + 2H_2\uparrow \quad (9)$$

The *in situ* hydrofluoric acid etching technique improves the quality of the produced MXene, allowing researchers to fabricate MXene in a range of sizes to accommodate different applications and requirements. A significant advantage of this method lies in the direct intercalation of fluoride ions between MXene layers, which enhances the stability of chemical reactions during etching. Additionally, it increases the specific surface area and the density of active oxidation sites. However, this method also has certain limitations, such as a prolonged drying process. Additionally, during the drying process, the interlayer spacing of MXene nanosheets may decrease or even collapse.

2.2. Electrochemical etching

Electrochemical etching [58], commonly conducted in HCl, produces a combination of -O, -OH, and -Cl terminal groups on the MXene surface. Yang *et al.* [59] successfully demonstrated the synthesis of $Ti_3C_2T_x$ MXenes via electrochemical corrosion. In certain instances, this etching process may result in the formation of carbon-derived carbides [60]. The results showed that the yield of double-layer or single-layer $Ti_3C_2T_x$ nanosheets can reach more than 90% [61]. Using this method, three MXenes, Ti_2CT_x, V_2CT_x, and Cr_2CT_x, were successfully fabricated and reported [51]. In the electrochemical process, the MAX phase reacts with chloride ions, leading to the formation of MXenes. Afterward, MXenes react with water and hydroxide ions, leading to the generation of hydroxide-terminated MXenes. This corrosion procedure can be outlined as follows:

$$Ti_3AlC_2 + 3Cl^- - 3e^- = Ti_3C_2 + AlCl_3 \quad (10)$$

$$Ti_3C_2 + 2OH^- - 2e^- = Ti_3C_2(OH)_2 \quad (11)$$

$$Ti_3C_2 + 2H_2O = Ti_3C_2(OH)_2 + H_2\uparrow \quad (12)$$

2.3. Hydrothermal synthesis

Hydrothermal synthesis is a method of preparing MXene materials by utilizing chemical reactions in aqueous solution under high temperature and high pressure conditions [62]. Hydrofluoric acid (HF) is a critical component in most MXene etching processes [63]. However, despite their effectiveness, some of these methods pose significant environmental hazards. The etching base used in these processes is highly reactive with amphoteric elements such as aluminum [64]. Nevertheless, traditional approaches have yet to achieve the synthesis of high-purity multilayer MXenes. One significant obstacle in producing MXenes through alkaline etching is the *in situ* development of oxide or hydroxide layers [65]. To address this, Li *et al.* [66] proposed a hydrothermal approach that utilizes NaOH to etch Ti_3AlC_2 (a MAX phase material) enabling the synthesis of $Ti_3C_2T_x$ MXenes. This process, illustrated in Figure 4(d), demonstrates that NaOH can effectively remove the aluminum layer at a temperature of 270°C, yielding MXenes with a reported purity of 92%. Additionally, Peng *et al.* [67] successfully prepared $Ti_3C_2T_x$ and Nb_2CT_x MXenes through a hydrothermal etching method assisted by a $NaBF_4$/HCl medium. The reaction process is shown in formulas (13) and (14):

$$2Ti_3AlC_2 + 2OH^- + 10H_2O = 2Ti_3C_2(OH)_2 + 2Al(OH)_4^- + 5H_2\uparrow \quad (13)$$

$$2Ti_3AlC_2 + 2OH^- + 10H_2O = 2Ti_3C_2O_2 + 2Al(OH)_4^- + 7H_2\uparrow \quad (14)$$

2.4. Artificial intelligence association synthesis

The Artificial Intelligence-Assisted Synthesis Method is an innovative method that combines advanced technology. By using artificial intelligence technologies such as machine learning and neural networks, researchers can analyze and model a large amount of experimental data to optimize the preparation parameters and processes of MXene. Specifically, the artificial intelligence model can predict the optimal reaction conditions and guide experimental design by learning the relationship between different preparation conditions and MXene performance, thereby improving preparation efficiency and material performance. For example, AI can help determine the optimal reaction temperature, time, reagent concentration and other parameters, reduce the number of experimental trial and error, and reduce costs. Wang *et al.* [68] utilized a back propagation neural network genetic algorithm (BPNN-GA) alongside response surface methodology (RSM) to optimize the hydrofluoric acid etching process for preparing Ti_3C_2 MXene from Ti_3AlC_2 with hydrofluoric acid. Compared to RSM, BPNN-GA exhibited significantly higher prediction accuracy for the preparation conditions, achieving superior metrics, including R^2(0.9830), MSE (2.6188), RMSE (1.6183), MAE (0.8504), and MAPE (0.0089%). After optimization by BPNN-GA, the ideal hydrofluoric acid concentration, etching time, and temperature were found to be 8.81%, 7.01 hours, and 45.07°C, respectively. Under these conditions, the removal rate of methylene blue (MB) by the prepared Ti_3C_2 MXene reached 99.39%. Analyses using XRD, SEM, TEM, XPS, Zeta potential, FTIR, and other techniques confirmed that Ti_3C_2 MXene features a two-dimensional crystal structure characterized by a multilayered configuration and functional surface termination groups. Zeta potential analysis revealed that the surface of Ti_3C_2 MXene maintains a negative charge over a broad pH range, making it highly effective for the adsorption of cationic dyes. The use of BPNN-GA provides important insights and innovative approaches for optimizing material preparation processes.

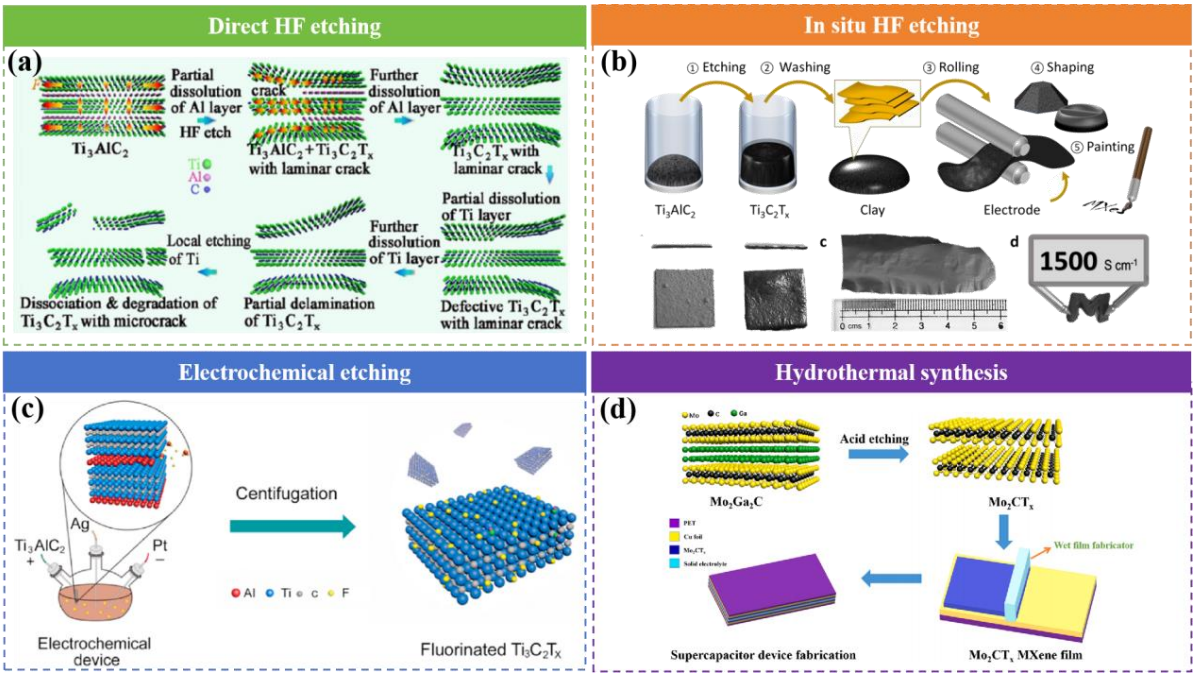

Figure 4. Major preparation method of MXene. **(a)** Direct HF etching. Reproduced from reference [52] with the permission of Elsevier. **(b)** In situ HF etching. Reprinted with permission [53]. Copyright 2014 Taylor & Francis eBooks. **(c)** Electrochemical etching. Reprinted with permission [58].

Copyright 2021 Elsevier. **(d)** Hydrothermal synthesis. Reprinted with permission [62] . Copyright 2021 Elsevier.

Zhao *et al.* [69] developed an annotated corpus that encapsulates domain-specific knowledge related to the synthesis processes of MAX and MXene materials. This dataset, compiled from the experimental sections of 110 research papers, was utilized to develop a baseline model incorporating named entity recognition (NER) and relation extraction (RE) modules. Utilizing a pre-trained natural language processing (NLP) framework, the model was constructed to identify and extract precise synthesis conditions described in scientific literature. The study demonstrated the effectiveness of this approach by combining domain expertise in MAX/MXene synthesis with advanced machine learning techniques. The optimized entity recognition model achieved an F1 score of 0.8452, while the relation extraction model achieved an F1 score of 0.8476. This work marks a significant advancement in applying NLP tools for comprehensive data extraction in the field of MAX/MXenes, with the potential to accelerate the development of these materials. Additionally, the model developed in this study could serve as a pre-trained foundation for future efforts in data augmentation and the extraction of MAX/MXene synthesis routes.

2.5. Other synthesis strategies

Various other synthesis methods, such as molten salt etching and ultrasonic exfoliation-assisted techniques, have also been employed to produce MXenes. Each of these methods provides distinct advantages and properties, making them suitable for specific applications.

2.5.1. Molten salt etching

Molten salt etching is a method of preparing MXene materials using molten salt as an etchant. This method selectively removes the A-layer elements in the MAX phase by mixing the MAX phase material with molten fluoride salt and reacting them under high temperature conditions to generate MXene with a two-dimensional layered structure. The advantage of this method is that it can be etched under acid-free conditions, reducing the use of acidic solutions in traditional wet etching. At the same time, the molten salt environment helps to control the interlayer spacing and surface chemical properties of MXene, so that it can exhibit excellent performance in electronic devices, energy storage materials, and electrocatalysis.

Arole *et al.* [70] proposed a technique to produce water-dispersed $Ti_3C_2T_x$ nanosheets was developed using molten salt etching with SnF_2. During this process, SnF_2 penetrates between the material's layers, leading to the formation of AlF_3 and Sn as byproducts, which facilitate the separation of the layers. The $Ti_3C_2T_x$ nanosheets formed a stable aqueous dispersion with a zeta potential of 31.7 mV, primarily due to the incorporation of -OH terminal groups during the KOH washing process. Analyses using X-ray diffraction and electron microscopy showed that $Ti_3C_2T_x$ etched via molten salt displays a larger d-spacing compared to that of HF-etched counterparts. This work represents the first successful preparation of a colloidally stable aqueous dispersion of $Ti_3C_2T_x$ nanosheets using molten salt etching technology.

2.5.2. Ultrasonic exfoliation-assisted

In the synthesis process of MXene, the ultrasonic exfoliation method is mainly used to exfoliate multilayer MAX phase materials into few-layer or single-layer structures. It is worth noting that the

ultrasonic exfoliation method does not directly participate in the etching process of the MAX phase, but is used to assist in the stripping after the initial etching, and further exfoliates the MAX phase material with the A layer removed into a thinner layered structure.

Yao *et al.* [71] developed a high-intensity ultrasonic exfoliation (HIUE) technique, significantly reducing the etching time to just 3 hours while achieving a yield of over 90% by optimizing parameters such as temperature, reagent dosage, and ultrasonic power. During the etching process, ultrasound facilitated the delamination of MXene, resulting in a one-step yield of 20% for low-layer MXene after centrifugation. The properties of MXenes produced using the HIUE method were compared with those prepared through traditional wet etching, revealing the former's efficiency. The practicality of the HIUE method was further confirmed through the fabrication of MXene-based nanocomposites and the assessment of their gas-sensing performance. The $Ti_3C_2T_x$ MXene produced using this method exhibited a reaction rate of 21.1% to 100 ppm NH_3, demonstrating good selectivity. Additionally, the MXene/MoS_2 nanocomposites produced using this swift preparation method demonstrated improved gas-sensing capabilities. These findings highlight the effectiveness and promise of the HIUE technique for the rapid synthesis of MXene-based materials.

2.6. Chapter summary

This section reviews the different preparation methods of MXene materials, including hydrofluoric acid preparation, electrochemical etching, hydrothermal synthesis, and artificial intelligence-assisted preparation, and briefly introduces several other preparation methods. These methods have their own characteristics and play an important role in the structural control, performance optimization, and application expansion of MXene.

The hydrofluoric acid-based preparation method is straightforward to perform and yields high-quality MXene materials, but the high corrosiveness and toxicity of hydrofluoric acid put forward high safety requirements for the experimental environment and operators. The advantage of the electrochemical etching method is that the interlayer spacing and thickness of MXene can be precisely controlled by regulating the voltage, electrolyte composition and reaction time. In addition, this method does not require the use of highly corrosive hydrofluoric acid, and the operation is safer and more environmentally friendly. However, the preparation efficiency of the electrochemical etching method is relatively low, and the equipment requirements are high. The hydrothermal synthesis method has the advantages of mild reaction conditions and large-scale preparation. At the same time, it can prepare MXene with different surface chemical properties and interlayer spacing by regulating the reaction conditions. However, the reaction time of the hydrothermal synthesis method is long and requires high equipment investment. The preparation of MXene by artificial intelligence-assisted preparation has the advantages of efficient optimization, intelligent monitoring and customized design. It can quickly determine the optimal preparation conditions through machine learning and data analysis, improve production efficiency and material performance; however, this method is highly dependent on a large amount of high-quality data and professional knowledge, there is a risk of data bias, and the model training is complex and the interpretability is poor. The initial investment cost is high, and the scope of application also needs further verification. This method represents the trend of deep integration of materials science and artificial intelligence, and has broad application prospects.

In summary, there are many methods for preparing MXene, each with its own advantages and limitations. In the future, with the continuous advancement of technology and the continuous optimization of methods, the preparation of MXene will be more efficient, safe and intelligent, promoting its wide application in various fields.

Table 1. Advantages and disadvantages of MXene synthesis methods.

Method	Advantages	Disadvantages
HF Etching	Simple to operate, produces high-quality MXene	Highly corrosive and toxic; requires safety measures
Electrochemical etching	Precise control of interlayer spacing and thickness; safer and environmentally	Low efficiency, high equipment cost
Hydrothermal synthesis	Mild reaction conditions, scalable production; adjustable surface	Long reaction time, requires high equipment investment
AI-assisted synthesis	Efficient optimization; Intelligent monitoring; Custom design	Dependence on high-quality data; complex model training; high cost

2. Preparation and properties of MXene membranes

MXene has several unique advantages over other 2D materials. Its excellent electronic and ionic conductivity, combined with its hydrophilic surface, makes it particularly suitable for applications such as energy storage and electronic devices. Unlike many other 2D materials, MXene can be easily functionalized by different surface functional groups such as -O, -OH and -F, resulting in tunable performance and improved adaptability for catalysis, sensing, and environmental applications. In addition, MXene exhibits high stability over a wide range of environmental conditions, allowing it to be used in a wider range of applications where high strength is required.

Various techniques are available for fabricating MXene-based membranes, including spraying, dip-coating, vacuum spin-coating, casting, layer-by-layer assembly, hot or cold pressing, electrospinning, deposition, and filtration [72]. This section focuses on discussing the casting, melt mixing, and vacuum-assisted filtration (VAF) techniques, while also providing a brief overview of several other methods used for MXene membrane preparation.

3.1. Vacuum filtration method

The preparation of MXene membranes by vacuum filtration is a simple and efficient method, especially suitable for the preparation of uniform and dense self-supporting membranes [73]. The basic steps of this method include: first, dispersing MXene powder in deionized water or other appropriate solvents, and ultrasonically treating to obtain a uniform MXene dispersion. Next, the dispersion is filtered through a vacuum filtration device, and a filter membrane with a suitable pore size (such as a polycarbonate membrane or a nylon membrane) is selected as the supporting material. During the filtration process, MXene flakes will gradually deposit on the surface of the filter membrane to form a dense membrane structure. Finally, the obtained MXene membrane is dried at room temperature or low temperature to obtain a complete MXene membrane.

The vacuum filtration method is simple to operate, easy to implement, and can produce uniform MXene films in a relatively short time. This method can produce dense, uniform, self-supporting MXene films with good mechanical strength, which are suitable for a variety of applications. In addition, the thickness of the film can be more accurately controlled by adjusting the concentration of the MXene dispersion and the filtration time. Ultrasonic treatment and vacuum filtration processes help to obtain well-dispersed MXene sheets, thereby improving the performance of the membrane.

It can be seen that the preparation of MXene membranes by vacuum filtration has many advantages, but there are also some disadvantages: (1) The vacuum filtration method is generally suitable for the preparation of small-area membranes and is difficult to achieve large-area or industrial-scale production; (2) It requires the use of equipment such as vacuum pumps and filter membranes, which increases the complexity and cost of the experimental setup; (3) The choice of filter membrane has a great influence on the quality of the final membrane. Different filter membranes may result in different membrane structures and properties; (4) Careful control of the drying process is essential to avoid membrane deformation or breakage, and removing the filter membrane can present additional challenges.

3.2. Casting method

Casting is a well-established method in membrane science for synthesizing membranes with precise compositions [74]. The process involves dissolving the membrane components in a solvent to create a uniform casting solution, which is then stirred or ultrasonicated to ensure thorough mixing. This solution is typically applied to a clean substrate for membrane formation. The phase inversion technique is commonly employed in conjunction with casting for membrane synthesis [75]. Given their hydrophilic nature, MXene materials interact favorably with hydrophilic polymers such as PVA, PEO, PEI, PU, and PAM, making them particularly suitable for membrane fabrication [76,77]. Figure 5 provides an overview of the casting process used to synthesize MXene-based membranes.

The casting method offers several advantages, such as excellent uniformity in film thickness, the absence of defects, and enhanced flexibility. However, the technique also presents some limitations: To ensure effective film formation, the polymer solution must dissolve in water or organic solvents, and its viscosity should be carefully optimized [78]. Although the casting method is economical, easy to perform, and efficient, a major challenge lies in avoiding the polymerization of MXenes during the procedure.

3.3. Electrospinning

Electrospinning is also an effective method for preparing MXene films. Through electrospinning technology, MXene can be mixed with polymer solutions, and the solution can be stretched into nanofibers using electrostatic force to form MXene films with excellent performance. This method helps to improve the uniformity and mechanical properties of the film, while also controlling the thickness and pore size distribution of the film. In the study, MXene films prepared by electrospinning also showed potential for application in energy storage, sensors, and filters.

Li *et al.* [79] prepared a series of sodium alginate/MXene composite nanofiber membranes by electrospinning and continuous ion-mediated crosslinking. The specific steps are as follows: sodium alginate aqueous solution, polyvinyl alcohol solution and MXene suspension are mixed to obtain a uniform and electrospinnable mixed solution; then the electrospinning solution is then placed into a

syringe and extruded through a stainless steel needle at a controlled rate onto a synthesis platform; then the resulting nanoparticles are soaked in a $CaCl_2$ solution at room temperature and thoroughly rinsed multiple times with deionized water; then, the prepared composite is immersed in deionized water at room temperature to eliminate any residual polyvinyl alcohol. Finally, it is removed and dried.

3.4. Artificial intelligence neural network

MXene films are prepared by using artificial intelligence (AI) neural networks and other means. Through the analysis and learning of a large amount of experimental data, the AI model can predict and optimize key parameters in the preparation process, such as temperature, time, pressure and solvent concentration, thereby improving preparation efficiency, reducing the number of trial and error, and achieving precise control and optimization of film performance. This method can not only ensure the consistency and excellent performance of the film, but also greatly reduce the experimental cost and promote the application of MXene films in electronics, energy and other fields.

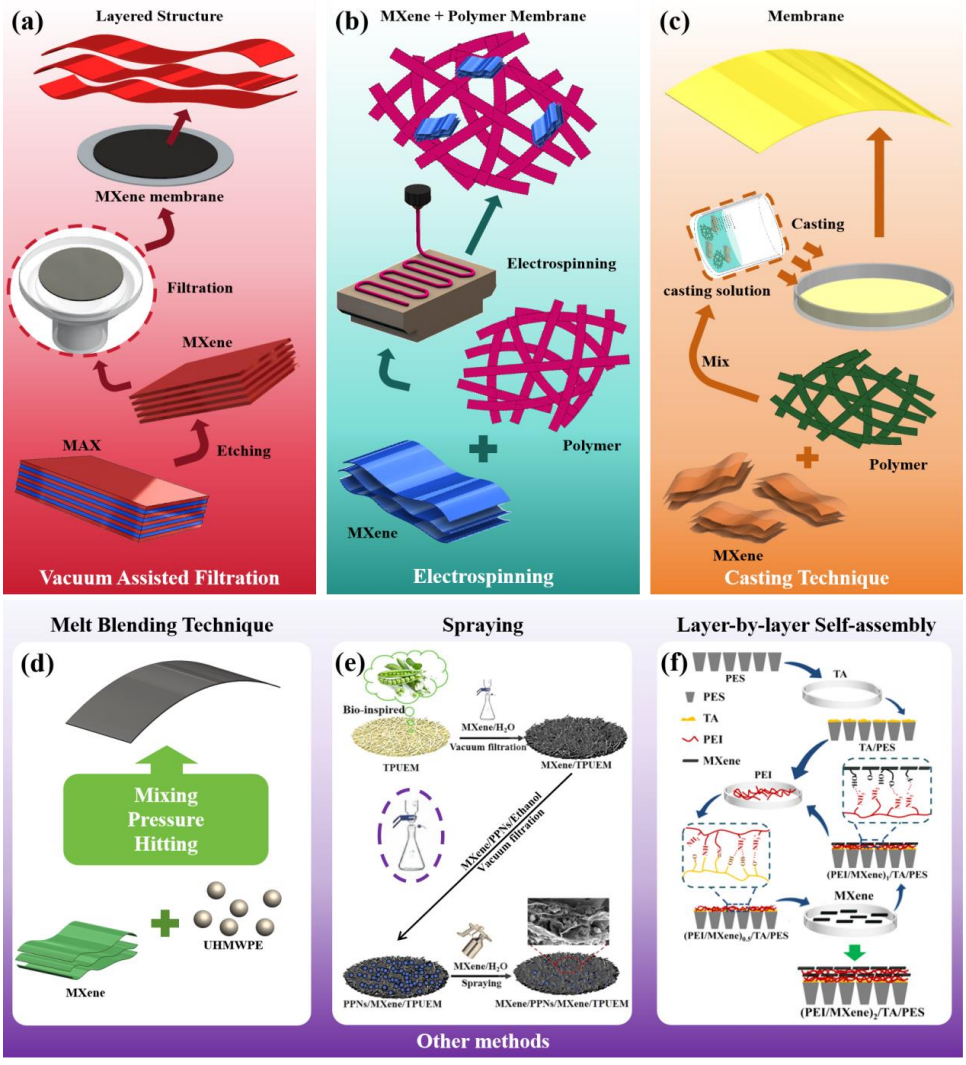

Figure 5. Preparation method of MXene film. **(a)** Vacuum Assisted Filtration. **(b)** Electrospinning. **(c)** Casting Technique. **(d)** Melt Blending Technique. **(e)** Spraying. Reprinted with permission [80]. Copyright 2023 Elsevier. **(f)** Layer-by-layer Self-assembly. Reprinted with permission [81]. Copyright 2023 Elsevier.

Ma *et al.* [42] employed a combination of machine learning (ML) techniques and global optimization algorithms to enhance the design of MXene membranes from various perspectives. Their study found that the particle swarm optimization (PSO) algorithm outperformed the genetic algorithm in terms of both convergence speed and stability. Through the application of PSO, $Ti_3C_2O_2$ with a specific charge at the nanopore mouth was identified as an optimal material candidate for membrane applications. By examining the water and ion densities within the nanopores, the research provided a detailed understanding of how pore charge and functional groups influence salt rejection and water permeability. The integration of machine learning with global optimization algorithms proved to be a powerful approach for designing materials with superior desalination performance.

3.5. Microwave-assisted hydrothermal etching

Microwave-assisted hydrothermal etching is an innovative MXene preparation technology that combines microwave heating with hydrothermal reaction to achieve efficient and uniform MXene etching in a short time. According to Purbayanto *et al.*, this method significantly shortens the reaction time during the conversion of Ti_3AlCN MAX phase materials into Ti_3CNT_x MXene while maintaining high-quality MXene structural properties [82]. In addition, this method significantly improves the photocatalytic performance of the material by generating TiO_2 crystals on the surface of the material, thereby greatly improving the degradation efficiency of organic pollutants such as methyl blue [83].

By optimizing the parameters such as microwave power, reaction temperature and time, this method can effectively control the layer spacing and surface functional groups of MXene, and enhance its application potential in the fields of energy storage and environmental management.

3.6. Other preparation methods

3.6.1. Molten salt

Zhang *et al.* [84] synthesized Ti_3C_2 nanomaterials and developed Ti_3C_2/ultra-high molecular weight polyethylene (UHMWPE) nanocomposites using a hot compression mold technique. The study demonstrated that the incorporation of Ti_3C_2 nanoparticles significantly enhances the thermal and mechanical properties of UHMWPE. Specifically, increases in Ti_3C_2 content were found to improve the crystallinity and hardness of the nanocomposites. Additionally, the tensile and fracture strengths were found to improve with increasing Ti_3C_2 content, peaking at a mass fraction of 0.75 wt.%. The inclusion of Ti_3C_2 also resulted in enhanced creep resistance. Further evaluation of the frictional properties using a pin-disc testing machine revealed that the Ti_3C_2/UHMWPE nanocomposites demonstrated enhanced friction-reducing performance compared to pure UHMWPE. The incorporation of Ti_3C_2 significantly minimized adhesive wear and friction, resulting in a smoother wear surface in the composites than that observed in pure UHMWPE.

3.6.2. Spraying method

Cheng *et al.* [80] designed a composite thermoplastic polyurethane electrospinning membrane (TPUEM) with a sandwich-like structure. This membrane incorporated MXene and poly(styrene-co-methacrylic acid)@polypyrrole nanospheres (PPNs) and was fabricated using a combination of vacuum filtration

and spraying methods. Initially, a MXene aqueous dispersion was prepared and subjected to ultrasonic treatment with a cell grinder to reduce the particle size of the MXene sheets. The fabricated TPUEM was placed on filter paper, and MXene dispersion was infused into it through vacuum filtration, resulting in the formation of the MXene/TPUEM composite. Following this, an ethanol dispersion containing MXene and PPNs was vacuum filtered through the MXene/TPUEM composite to create the PPNs/MXene/TPUEM structure. Finally, an additional layer of the MXene aqueous solution was sprayed onto the surface of the PPNs/MXene/TPUEM composite using a spray gun. The composite material exhibited superior electromagnetic shielding properties due to the intrinsic shielding capabilities of MXene and the unique sandwich structure. This suggests that the MXene/PPNs/MXene/TPUEM composite is highly effective in reducing electromagnetic interference from surrounding circuits and microelectronic components. Additionally, The pressure sensor constructed using the MXene/PPNs/MXene/TPUEM composite exhibited outstanding negative piezoresistive characteristics, such as high sensitivity, an extensive sensing range, and rapid response time. Moreover, the sensor showed exceptional capability in accurately monitoring various human activities, such as joint flexion, sound recognition, and pulse detection. These findings suggest that the MXene/PPNs/MXene/TPUEM composite holds significant potential for the development of multifunctional smart wearable devices.

3.6.3. Layer-by-layer self-assembly

Hu *et al.* [81] successfully developed a nanofiltration membrane for efficient dye wastewater treatment using layer-by-layer (LBL) self-assembly technology. The method involves sequentially assembling MXene and polyethyleneimine (PEI) on a polyethersulfone (PES) substrate and assembling through a tannic acid (TA) coating derived from plant polyphenols. They immersed the PES membrane in a PEI solution to fill the membrane with PEI, and then immersed it in a MXene dispersion to allow MXene and PEI to self-assemble on the PES substrate. These two steps were repeated to achieve layer-by-layer self-assembly of PEI and MXene.

3.7. Chapter summary

This section provides a detailed discussion on the preparation of MXene films using methods such as vacuum filtration, casting, electrospinning, and artificial intelligence-based neural network approaches. These methods have their own characteristics and provide a variety of options for the preparation of MXene films.

The advantage of the vacuum filtration method is that it can produce films with uniform thickness, low porosity and excellent conductivity. In addition, the vacuum environment helps to remove solvents and impurities, and improve the purity and performance of the film. This method is widely used in electronic devices, supercapacitors and batteries. However, its preparation speed is relatively slow, which is suitable for laboratory research and small-scale production, and there are certain challenges in large-scale industrial applications. The casting method offers several advantages, including ease of operation, cost-effectiveness, and suitability for producing large-area films. However, the thickness and uniformity of the film are difficult to accurately control, and the mechanical properties and conductive properties may be affected by the preparation conditions. Despite this, the casting method is still a common method for preparing MXene films, especially when rapid prototype preparation or preliminary

experiments are required. Electrospinning has a wide range of applications in sensors, filter membranes and catalysts. Since the fiber diameter is controllable, the pore structure and thickness of the film can also be precisely adjusted. However, the electrospinning equipment is complex and has high requirements for process parameters. The preparation process may be affected by environmental humidity and temperature and needs to be carried out under strictly controlled conditions. The preparation of MXene films by artificial intelligence neural network is a method that combines advanced AI technology to optimize the preparation process. The advantages of this method are that it significantly improves preparation efficiency, reduces the number of trial and error, reduces experimental costs, and achieves precise control and optimization of film properties. However, this method is highly dependent on a large amount of high-quality data and advanced computing resources, and places high demands on the interdisciplinary expertise of the research team.

In summary, vacuum filtration, casting, electrospinning and artificial intelligence neural network methods have their own advantages and limitations in the preparation of MXene films. By combining the characteristics of different methods and optimizing and improving them according to specific application requirements, MXene films with excellent performance and wide application can be prepared, promoting their wide application in electronics, energy, environment and other fields.

Table 2. Advantages and disadvantages of MXene membrane preparation.

Method	Advantages	Disadvantages
Vacuum filtration method	Produces films with uniform thickness,low porosity, excellent conductivity; vacuum improves purity and performance	Slow preparation speed; suitable for lab research and small-scale production; challenging for large-scale applications
Casting method	Simple operation, low cost, suitable for large-area film preparation	Difficult to control thickness and uniformity; mechanical and conductive properties affected by conditions
Electrospinning	Controllable fiber diameter; precise adjustment of pore structure and thickness	Complex equipment; high requirements for process parameters; sensitive to humidity and temperature
Artificial Intelligence Neural Network	Significantly improves preparation efficiency, reduces trial and error, minimizes experimental costs, achieves precise control and optimization	Requires large amounts of high-quality data and advanced computing resources; demands interdisciplinary expertise
Microwave-assisted hydrothermal etching	Rapid reaction; enhanced material performance	High equipment requirements; dependence on precise parameter optimization

4. Mechanism of the influence of interlayer spacing regulation on ion exchange membrane performance

4.1. Anion exchange membrane transport mechanism

When the ion exchange membrane carries a fixed negative charge, the membrane is called an anion exchange membrane (AEM). The anion electrolyzer is mainly composed of three parts: a gas diffusion layer, a catalyst layer, and an anion exchange membrane, as shown in Figure 6(a). During the electrolysis

process, water molecules undergo an oxidation reaction at the anode (positive electrode) to produce oxygen (O_2), hydroxide ions (OH^-) and electrons (e^-), while hydroxide ions (OH^-) accept electrons at the cathode (negative electrode) to undergo a reduction reaction to produce hydrogen (H_2) and water [85]. During this process, hydroxide ions (OH-OH^-OH-) move through the electrolyte from the cathode to the anode, ensuring the continuation of the reaction [86]. The high selectivity and high conductivity of the anion exchange membrane ensure that hydroxide ions can pass through the membrane quickly and effectively, thereby enhancing the overall efficiency of hydrogen production through water electrolysis [87]. Its working principle can be expressed by the following formula:

$$\text{Cathode}: 2H_2O + 2e^- \rightarrow H_2 \uparrow + 2OH^- \left(E^0 = -0.83\text{V } \textit{vs.}\ \text{SHE}\right) \quad (15)$$

$$\text{Anode}: 2OH^- \rightarrow \frac{1}{2}O_2 + H_2O + 2e^- \left(E^0 = 0.40\text{V } \textit{vs.}\ \text{SHE}\right) \quad (16)$$

$$\text{Overall}: H_2O \rightarrow H_2 \uparrow + \frac{1}{2}O_2 \uparrow \left(E^0 = -1.23\text{V } \textit{vs.}\ \text{SHE}\right) \quad (17)$$

Since most of the cationic groups are connected to the polymer skeleton of AEM through covalent bonds, these cationic groups can attract and fix hydroxide ions because of their opposite charge to hydroxide ions. This behavior enables the free transfer of hydroxide ions in the membrane. At the same time, due to hydration, hydroxide ions combine with water in the membrane to form hydrated ions. This series of hydrated ions forms a hydrogen bond network through hydrogen bonds. Hydroxyl ions jump in the hydrogen bond network through the Grotthuss mechanism, allowing the rapid transfer of hydroxide ions [88], as shown in Figure 6(b). In addition, the transfer of hydroxide ions in the membrane is also affected by diffusion mechanism, permeation mechanism, and electromigration mechanism. Among them, the permeation mechanism refers to the transfer of hydroxide ions of hydroxide ions through the membrane under the action of concentration gradient. This mechanism is affected by factors such as membrane permeability, membrane thickness, and concentration gradient of hydroxide ions in the electrolyte.

An optimal anion exchange membrane (AEM) should feature a robust matrix with continuous ion-conducting channels extending throughout the membrane. This design ensures efficient ion transport while preserving structural integrity and stability, particularly in alkaline and aqueous environments. In comparison to acidic proton exchange membranes (PEMs), anion exchange membranes (AEMs) generally demonstrate lower conductivity. This is primarily due to the inherently low mobility of hydroxide ions and the limited basicity of the cationic sites [89–91]. The ionic conductivity of anion exchange membranes (AEMs) is significantly affected by various factors, including ion exchange capacity (IEC), the mobility of ions, hydration levels, and the membrane's micromorphology [92–94]. By adjusting the interlayer spacing between MXene nanosheets in MXene-based ion exchange membranes, it is possible to optimize the ion transport rate, transfer pathways, permselectivity, as well as the mechanical properties and chemical stability of the membrane to varying degrees, as shown in Figure 6(c).

4.2. Ion transmission rate and transfer path

Interlayer regulation plays a crucial role in influencing both the ion transfer path and the conductivity of exchange membranes. By adjusting the interlayer spacing of two-dimensional materials like MXene, the ion transfer path within the membrane can be effectively controlled. When the interlayer spacing is optimal, ions can smoothly pass through the interlayer gap, creating a stable transmission channel.

However, if the spacing is too large or too small, it can hinder ion transfer and reduce conduction efficiency. The stacking method also impacts the ion transfer path. For instance, regular stacking results in a relatively linear and straightforward ion transfer path, whereas random stacking or staggered arrangements create more complex paths, which may enhance ion selectivity. Changes in interlayer spacing directly influence the diffusion rate of ions through the membrane. A larger interlayer spacing can decrease the interaction between ions and membrane materials, allowing ions to traverse the membrane layer more rapidly, thereby improving conductivity. However, if the spacing is too large, ions may become "trapped" in the membrane, ultimately reducing conductivity. Furthermore, regulating interlayer spacing affects the adsorption and distribution of water molecules, which in turn influences the hydration state and mobility of ions. In certain cases, an optimal interlayer spacing can promote water molecule retention, thereby improving ion hydration and enhancing ionic conductivity.

Hatakeyama *et al.* [95] investigated how interlayer spacing and the quantity of oxygen functional groups influence ion permeation through graphene oxide (GO) membranes. The study revealed a strong linear correlation between the ion permeability of GO and its interlayer spacing, which remained consistent even when the spacing was modified using various techniques. By controlling the interlayer distance, the permeability of GO was $0 \sim 2 \mathrm{mol} \cdot \mathrm{h}^{-1} \cdot \mathrm{m}^{-2}$ successfully adjusted within Cu^{2+} a range.

4.3. Selective permeability

Ren [96] *et al*. reported the selective screening of alkali, alkaline earth, transition metal, and methyl sulfide ion dye cations through $Ti_3C_2T_x$ membranes. Their study found that the interlayer spacing of $Ti_3C_2T_x$ increases with rising water content. The calculated interlayer distances at 140 °C, 70 °C, and under wet conditions were 2.9 Å, 4.7 Å, and 6.4 Å, respectively, corresponding to one, two, and three layers of water molecules between the $Ti_3C_2T_x$ sheets. These three water layers create an unrestricted pathway for water transport, facilitating the generation of high water flux.

Wu *et al.* [97] designed a 2 μm thick MXene film made of stacked $Ti_3C_2T_x$ nanosheets, which was utilized for ethanol dehydration applications. To elucidate the separation mechanism, the MXene film was immersed in water, ethanol, and isopropanol. XRD analysis reveals that the characteristic peak of the dry MXene film appears at 6.4°, corresponding to a calculated d-spacing of 1.37 nm. According to previous studies, the theoretical thickness of a single-layer MXene nanosheet is about 1.0 nm [63,98], the interlayer distance within the MXene film was calculated to be 0.37 nm. Upon immersion in water, the XRD peak shifted to 5.7°, indicating an increase in d-spacing by 0.23 nm. Further analysis showed that after 2 hours of immersion in water, the d-spacing increased by 0.2 nm. After the film was immersed in pure water for 5 days, it was found that the increase in its d-spacing was still around 0.2nm, which shows that the MXene film has a certain stability in a pure water environment. In contrast, when the MXene film was immersed in ethanol, the XRD peak showed no significant shift compared to the dry film, indicating strong anti-swelling properties in ethanol. Moreover, the anti-swelling performance of the MXene film improved with higher ethanol concentrations, maintaining an interlayer spacing of approximately 0.42 nm. Given the dynamic diameters of water (0.29 nm) and ethanol (0.45 nm) molecules, these results suggest that the MXene film can effectively separate water from ethanol through a molecular sieving mechanism.

4.4. Mechanical properties and chemical stability

In the practical application of MXene membranes, environmental stability is one of the key factors, including humidity, temperature, and oxidation stability. Existing studies have shown that changes in humidity and temperature can significantly affect the conductivity and structural stability of MXene films. For example, Ti_3CNT_x films are prone to degradation in environments with high humidity, which limits their lifetime in real-world environments. To solve this problem, a strategy of coating the surface of the film with a reduced graphene oxide (rGO) layer can be adopted, which helps to improve the stability of the MXene film in a high humidity environment [82].

Ding *et al.* [99] developed an MXene (MXMA) membrane by depositing it onto a microporous nylon matrix using vacuum-assisted filtration synthesis technology, and explored its efficacy in pervaporation desalination. The MXene nanosheets within the membrane were securely bonded through covalent linkages formed by esterification reactions between the carboxyl groups in maleic acid and the hydroxyl groups on the surface of the MXene. These covalent bonds provided strong interlayer connections within the cross-linked MXMA membrane, significantly enhancing its anti-swelling properties and overall stability. The study demonstrated that the change in d-spacing for the MXene membrane after soaking in deionized water was 31.4%, whereas the cross-linked MXMA membrane exhibited only a 2.7% change. This indicates that the MXene nanosheets in the MXMA membrane were effectively stabilized by the covalent bridges formed with maleic acid, which substantially inhibited interlayer expansion and improved the mechanical strength of the membrane.

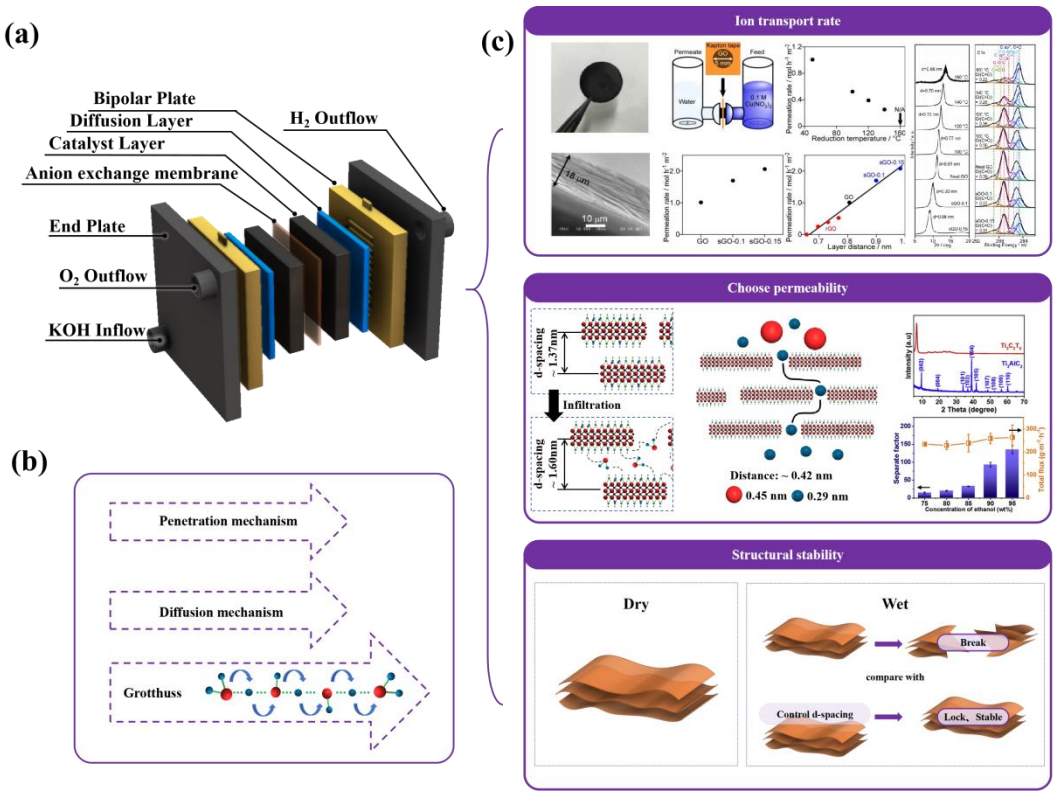

Figure 6. (a) Anion electrolyzer structure; **(b)** Grotthuss mechanism; **(c)** effect of interlayer spacing on ion transport rate and transfer path, permselectivity, and mechanical properties and chemical stability of the membrane. Reprinted with permission [95,97]. Copyright 2017 Elsevier. Copyright 2019 Elsevier.

4.5 Chapter Summary

This section focuses on the effect of interlayer spacing regulation on the performance of ion exchange membranes. By regulating the interlayer spacing of MXene, the ion conductivity, selective permeability, and mechanical and chemical stability of the membrane can be significantly affected. First, appropriate interlayer spacing can form efficient ion channels, optimize ion conduction paths, and improve the conductivity of anions, which is crucial to improving the performance of AEM in electrochemical devices such as fuel cells. Secondly, by regulating the interlayer spacing, channels with selective permeability can be constructed to achieve highly selective separation of specific anions and enhance the separation effect of the membrane. In addition, reasonable interlayer spacing regulation helps to enhance the mechanical strength of the membrane, enabling it to maintain structural integrity under high pressure conditions, while improving the chemical stability of the membrane and extending its service life. These optimization effects make MXene interlayer spacing regulation show broad application prospects in the fields of water electrolysis for hydrogen production and thin-film fuel cells.

5. MXene film interlayer spacing control strategy

The regulation of interlayer spacing in MXene nanosheets within MXene-based anion exchange membranes can be effectively achieved through several key strategies: surface functionalization, intercalation chemistry, nanomaterial composites, and polymer composites. Surface functionalization involves the introduction of functional molecules or groups onto the surface of MXene nanosheets, which modulates the interlayer interactions [63]. By inserting small molecules between MXene layers, this method forms intermolecular forces, such as hydrogen bonds or ionic bonds, which can either increase or decrease the interlayer spacing to enhance the membrane's ion conduction properties [98]. Intercalation chemistry allows for the insertion of various species between the layers of MXene, thereby fine-tuning the spacing for optimal performance [99]. The use of nanomaterial composites involves incorporating other nanomaterials with MXene nanosheets, which adjusts the interlayer spacing through a combination of physical filling and chemical interactions. This method provides a synergistic approach to enhancing membrane performance by leveraging the unique properties of different nanomaterials. Polymer composites, on the other hand, combine MXene nanosheets with polymers. This strategy uses interfacial forces and space-filling effects to regulate the interlayer spacing, providing a balance between flexibility and structural stability in the resulting membrane. Each of these strategies offers distinct advantages in tailoring the interlayer spacing of MXene nanosheets, thereby enabling precise control over the membrane's ion conduction performance.

5.1. Surface functionalization

By introducing different functional groups (such as -OH, -O, -F) on the surface of MXene, the interlayer electrostatics and van der Waals forces can be changed, thereby adjusting the interlayer spacing. Different chemical environments and processing conditions can control the number and type of these groups, making the interlayer spacing more precisely regulated.

Berdiyorov *et al.* [100] utilized density functional theory (DFT) calculations to explore how surface functionalization influences the interaction of bilayer $Ti_3C_2T_x$ MXene with intercalated ions. For

unmodified MXene, interlayer spacing expands with the addition of anions and cations. However, after functionalization, the system's behavior changes notably: anion intercalation increases the spacing, whereas cation intercalation reduces it. As the charge state of the cations increases, the interlayer spacing decreases further, and this effect is more pronounced in the case of $Ti_3C_2O_2$. Molecular dynamics simulations based on DFT and ReaxFF force fields also confirmed the dynamic response of the system to intercalated ions. These findings highlight the critical role of surface functionalization in optimizing MXene for water-related applications. Ibragimova *et al.* [101], employing a multiscale computational approach, unveiled the distribution and composition of O, OH, and F terminations on MXene surfaces, highlighting their significant impact on conductivity and work function. The study also emphasized the crucial role of environmental factors, such as pH, in modulating surface characteristics. In parallel, Du *et al.* [102] explored the synergistic optimization of interlayer spacing and surface terminations in Ti_3C_2Tx MXenes through alkali treatments, achieving enhanced electromagnetic wave absorption by balancing conductivity and impedance matching. Collectively, these studies underscore the critical importance of precise control over MXene surface chemistry and structural parameters, opening new avenues for innovations in energy storage, catalysis, and electromagnetic applications.

In their latest study, Dahlqvist *et al* [103]. delve into the pivotal role of sulfur and halogen surface terminations in shaping the structure, stability, and properties of MXenes—an extraordinary class of two-dimensional (2D) materials. As a family of transition metal carbides, nitrides, and carbonitrides, MXenes exhibit remarkable tunability, with their electronic, mechanical, and chemical behaviors being significantly influenced by their surface terminations. Employing density functional theory (DFT), the study investigates the effects of termination coverage, ranging from complete (100%) to partial (50%). The findings reveal that while suboptimal termination coverage can enhance electronic conductivity, it often compromises structural stability. Additionally, the analysis of interlayer binding energies highlights the challenges of delaminating MXenes with non-ideal surface terminations, particularly those involving halogen or sulfur species. This work offers profound insights into tailoring MXene properties for applications in catalysis, energy storage, and advanced electronics, emphasizing the importance of precise control over surface chemistry and termination coverage.

5.2. Intercalation chemistry

Inserting molecules or ions between MXene sheets to adjust the interlayer spacing is currently a widely used method to adjust the interlayer spacing of MXene. After intercalation, different intermolecular forces are formed to form different crosslinking forms, which can be divided into: hydrogen bond crosslinking, ionic bond crosslinking, and chemical bond crosslinking. In addition, there are some other types of crosslinking forms, which are also briefly introduced in this section in combination with practical applications.

5.2.1. Hydrogen bonding cross-linking

Wang *et al.* [104] used a magnetic hydrothermal synthesis method to construct a three-dimensional interconnected network of 1T-MoS_2/Ti_3C_2 MXene heterostructure and studied its electrochemical storage mechanism. Due to the synergistic interaction effect in the 3D interconnected network, the ion storage space is expanded, so an improvement in additional capacitance can be observed. The d-spacing of the

XRD results was calculated using the Bragg formula. The results show that the d-spacing of MoS_2 on the surface of Ti_3C_2 MXene prepared under zero magnetic field and 9T magnetic field is respectively ≈ 6.3 Å and 9.4 Å. The excellent rate performance is achieved due to the ultrafast electron transfer of Ti_3C_2 MXene.

5.2.2. Ionic bond crosslinking

In addition to regulating the interlayer spacing by forming hydrogen bonds by inserting molecules between layers, researchers have found that inserting ions between MXene sheets can also control the interlayer spacing, and most ion intercalation will result in a smaller interlayer spacing, which is the opposite of hydrogen bond regulation.

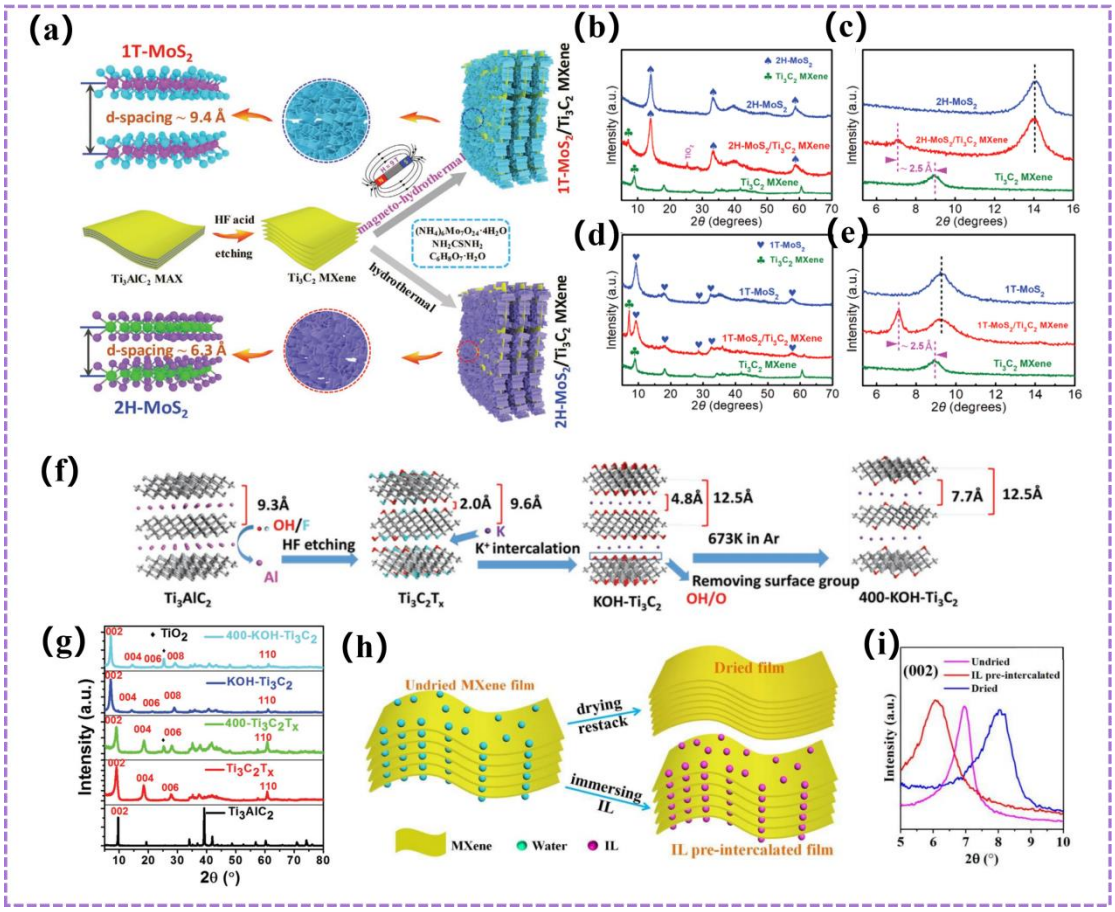

Figure 7. Controlling the interlayer spacing of MXenes through hydrogen and ionic bonds. **(a~e)** Reproduced from reference [102] with the permission of Wiley. **(f,g)** Reproduced from reference [103] with the permission of Elsevier. **(h,i)** Reproduced from reference [106] with the permission of RSC.

Li *et al.* [105] developed a method to substantially improve the performance of $Ti_3C_2T_x$ MXenes through cation insertion and surface modification, with a focus on enhancing gravimetric capacitance. After the insertion and subsequent removal of terminal groups, MXene samples treated with various cationic bases (NH_4OH, LiOH, NaOH) exhibited similar 002 peak positions, corresponding to interlayer distances of approximately 12.7 Å, 12.6 Å, and 12.4 Å, respectively. These comparable interlayer distances are likely a result of differing degrees of cation solvation between the Ti_3C_2 layers, combined with the presence of water, which serves to mitigate the effects of cation size. The modified MXenes

demonstrated a threefold increase in insertion pseudocapacitance compared to the unmodified material, leading to a significant enhancement in the gravimetric capacitance of the MXene flakes. Furthermore, the fabricated electrode maintained over 99% of its performance after 10,000 cycles, indicating excellent long-term stability. This notable improvement in electrochemical performance is attributed to the increased interlayer spacing in Ti_3C_2 and the reduced concentration of terminal surface groups, which together optimize the material's capacitance properties.

Zheng *et al.* [106] reported the fabrication of advanced high-voltage ion gel-based micro-supercapacitors (MSCs) integrated on-chip, utilizing interdigital microelectrode fingers pre-intercalated with MXene films in ionic liquids. This method significantly enhances volumetric energy density and flexibility while enabling the modular integration of bipolar batteries. The interdigital microelectrodes, produced by depositing MXene and graphene with the aid of an interdigital mask, demonstrate exceptional conductivity of 2200 $S \cdot cm^{-1}$. This exceptional conductivity is realized without the use of polymer binders, conductive additives, or metal current collectors. The pre-intercalation of ionic liquid into MXene-based electrode films establishes a continuous ion transport network, increasing the interlayer spacing to 1.45 nm—surpassing that of undried MXene (1.27 nm) and fully dried MXene (1.09 nm).

5.2.3. Covalent cross-linking

In order to form stable covalent crosslinks between MXene layers, small molecules, such as amines and alcohols, are generally subjected to amidation or esterification reactions with hydroxyl and carboxyl groups on MXene. Covalent bonds are formed through these chemical reactions to connect MXene nanosheets. This method can not only improve the hydrophilic/hydrophobic properties of MXene films, adjust the interlayer spacing of the films, but also improve the mechanical strength of the films, and even improve the electrical conductivity and ionic conductivity of the films.

Ding *et al.* [99] employed vacuum-assisted filtration synthesis technology to create a maleic acid covalently bridged MXene membrane supported on nylon (polyamide) microfiltration membranes. Adjacent MXene nanosheets were securely bonded together by covalent bonds formed through esterification between the carboxyl groups in maleic acid and the hydroxyl groups on the MXene surface. As depicted in the figure, the cross-sectional SEM image of the cross-linked membrane reveals an ordered layered structure, with the interlayer spacing of this structure providing a two-dimensional transmission channel for molecular transport. To further investigate the interlayer structure of the membrane, the crystal structure and d-spacing of the MXene maleic acid cross-linked membrane and the pure MXene membrane were analyzed using XRD, as shown in Figure 10(a) and Figure 10(b). The calculated interlayer spacing of the pure MXene membrane is approximately 0.37 nm, consistent with previous studies [107]. The interlayer spacing of the maleic acid MXene cross-linked membrane was calculated to be 0.49 nm. This increase in interlayer spacing indicates that maleic acid has successfully cross-linked the MXene nanosheets via covalent bonds. Due to the excellent hydrophilicity of MXene nanosheets, water molecules can infiltrate the interlayer space in an aqueous environment, causing the MXene film to swell and thereby reducing its mechanical properties. To assess the mechanical stability of the MXene maleic acid film in water, it was pre-soaked in deionized water for up to 24 hours. The test results show that the d-spacing of the pure MXene film expanded by 31.4% to 1.80 nm, resulting in an interlayer size of 0.80 nm. In contrast, the expansion rate of the MXene maleic acid cross-linked film was only 2.7%, indicating that the MXene nanosheets in the MXene maleic acid cross-linked film are

covalently cross-linked with maleic acid through surface functional groups, effectively inhibiting the expansion of the interlayer spacing and enhancing the mechanical strength of the film.

Xing *et al.* [108] developed a CTS-MXene/PAN membrane by vacuum filtering a mixed suspension of chitosan at various concentration gradients and a fixed concentration of 1 mg/mL MXene $Ti_3C_2T_x$ onto a PAN nanofiber substrate at 0.2 MPa. The structure and composition of the resulting membrane were characterized using X-ray photoelectron spectroscopy (XPS). Analysis of the C1s peak identified a CN peak at 287.3 eV, confirming the formation of covalent bonds between the chitosan (CTS) and MXene [109,110].Further characterization using X-ray diffraction (XRD) revealed that the interlayer spacing of the MXene/PAN membrane was 15.20 Å. In contrast, the interlayer spacing of the CTS-MXene/PAN membrane decreased slightly to 14.33 Å. This reduction in interlayer spacing is attributed to the formation of CN covalent bonds between CTS and $Ti_3C_2T_x$, which enhances the membrane's selective permeability, improves its mechanical strength, and extends its operational lifespan.

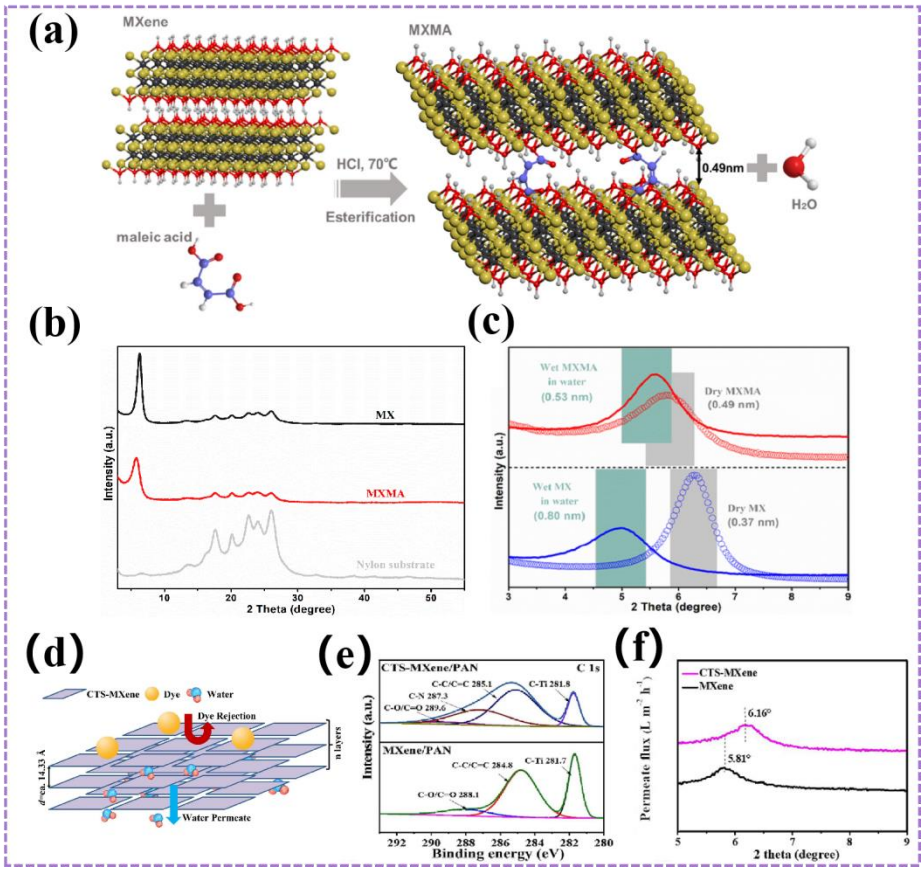

Figure 8. Tuning the interlayer spacing of MXenes via covalent crosslinking. **(a,b,c)** Reprinted with permission [99]. Copyright 2020 Elsevier. **(d,e,f)** Reprinted with permission [108]. Copyright 2023 Elsevier.

5.2.4. Cross-linking by combination of multiple intermolecular forces

By integrating hydrogen and ionic bonds for crosslinking, the interlayer spacing of MXene membranes can be optimized to achieve superior structural stability and functional properties. Hydrogen bonds contribute to flexibility and reversibility, while ionic bonds enhance mechanical strength and conductivity. This synergistic interaction improves the membrane's durability and versatility without

compromising its flexibility, thereby expanding its potential applications across various fields, including water treatment, supercapacitors, and flexible electronic devices.

Wan *et al.* [111] introduced an innovative method for producing robust and highly conductive MXene sheets by sequentially incorporating hydrogen and ionic bonds. The ionic bonding agent reduced the interlayer spacing of the MXene nanosheets and enhanced their alignment, whereas the hydrogen bonding agent increased the spacing and reduced alignment. This sequential bonding approach optimized key properties of the MXene sheets, including toughness, tensile strength, resistance to oxidation in humid conditions, durability against sonic decomposition, and mechanical stress resilience. The resulting MXene sheets demonstrated remarkable mechanical and electrical properties, with a tensile strength of up to 436 MPa, electrical conductivity as high as 2988 S/cm, and a weight-normalized shielding efficiency of 58929 dB·cm²/g. The underlying toughening and strengthening mechanisms were further elucidated through molecular dynamics simulations. This sequential bonding strategy provides a valuable approach for assembling other high-performance MXene-based nanocomposites.

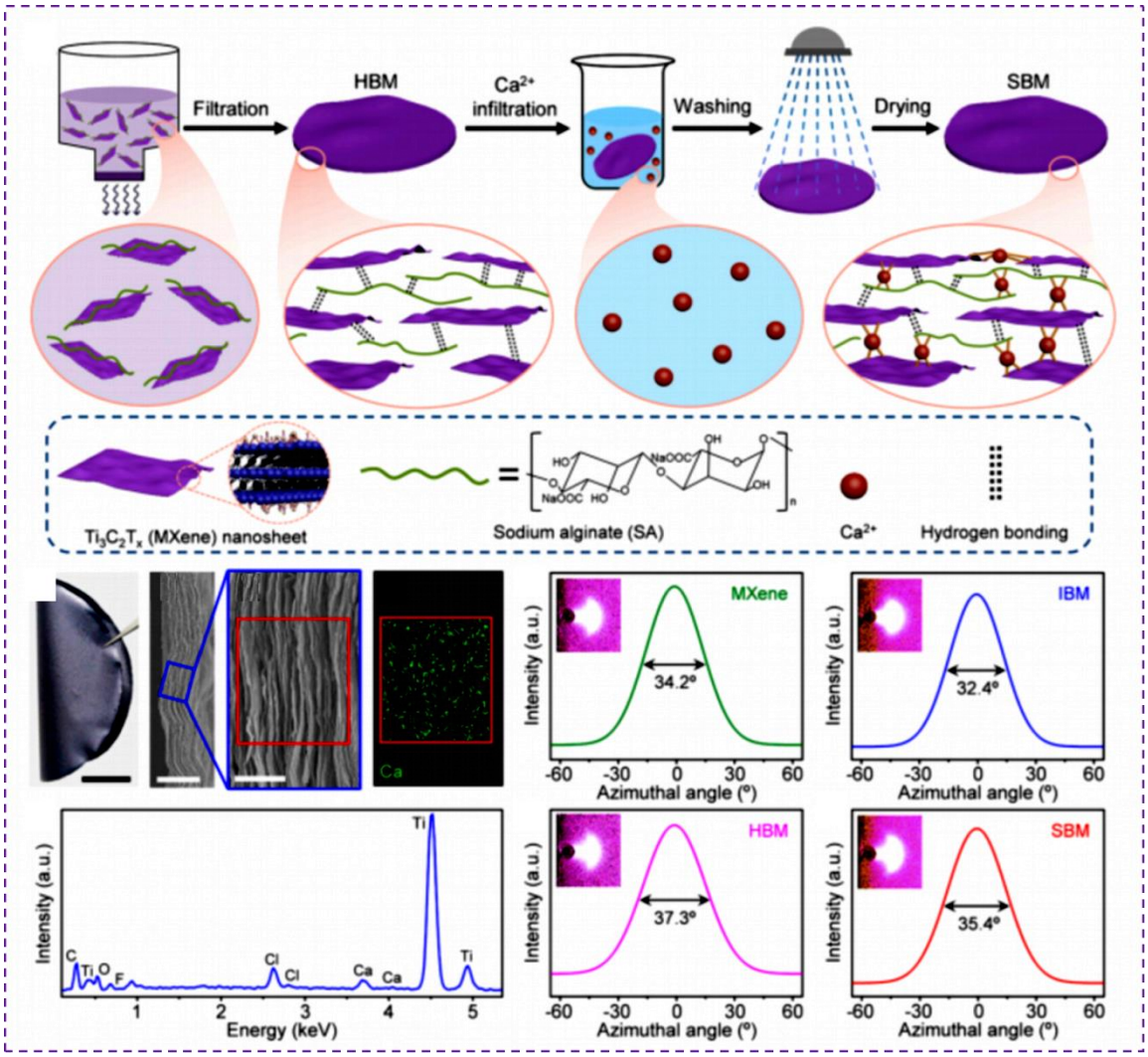

Figure 9. Sequential bridging of MXene sheets via hydrogen and ionic bonds regulate interlayer spacing. Reprinted with permission [111]. Copyright 2020 Elsevier.

The inherent mechanical brittleness and oxidative susceptibility of MXene materials significantly limit their potential for widespread application. To overcome these limitations, Shilu Luo *et al.* [112]

proposed a dual cross-linking strategy that successfully addresses these challenges by forming a bead-like "brick-and-mortar" layered MXene/cellulose structured (MXene/CNF) film. In this approach, MXene was initially modified with dopamine, a modification that not only enhanced the antioxidant properties of MXene but also promoted hydrogen bonding interactions with CNF. Following this, the modified MXene was incorporated *in situ* into a layered composite film produced through filtration, leading to the formation of additional ionic bonds between CNF and MXene. The dual cross-linking approach proved to be substantially more effective in enhancing the composites mechanical properties than traditional single cross-linking techniques. The mechanical strength and toughness of the dual cross-linked MXene/CNF film were enhanced to 142.2 MPa and 9.48 MJ/m³, respectively. Moreover, the MXene composite film maintained excellent electromagnetic interference (EMI) shielding performance, exceeding 44.6 dB, even after undergoing high-temperature annealing and oxidation treatments. This stability underscores the film's robust antioxidant capabilities and environmental resilience.Overall, this study presents a versatile and effective dual cross-linking strategy to mitigate the mechanical brittleness and oxidative instability of $Ti_3C_2T_x$-based composites, highlighting its significant potential for flexible EMI shielding applications.

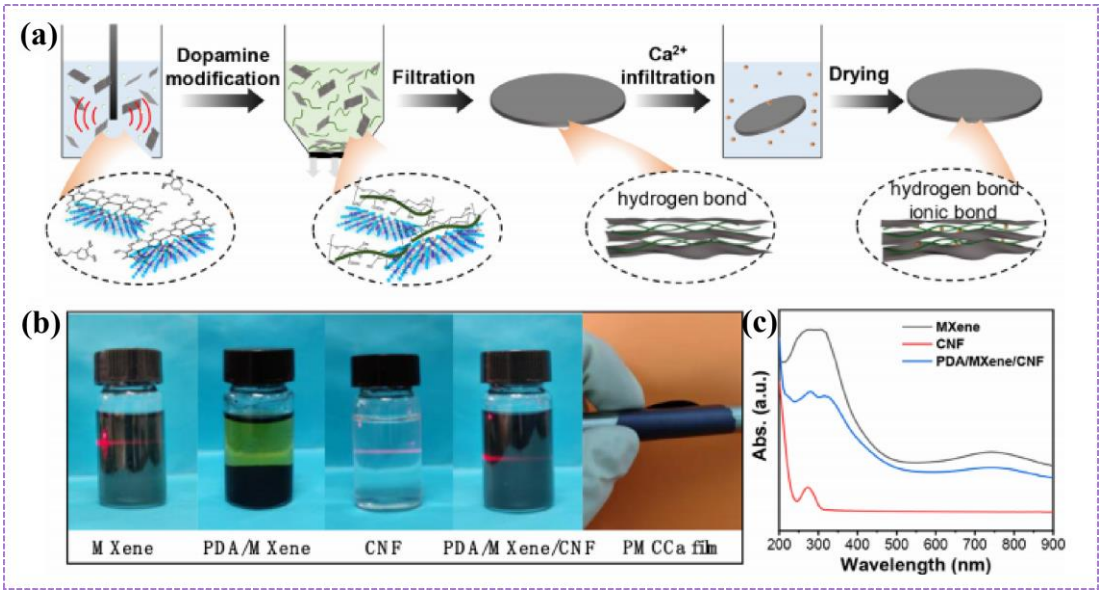

Figure 10. Modification of MXene by dopamine hydrogen bonding and insertion Ca^{2+} of ionic bonds regulate interlayer spacing. Reprinted with permission [112]. Copyright 2022 Elsevier.

Wan [113] introduced an effective densification strategy for $Ti_3C_2T_x$ MXene films through a sequential bridging process that incorporates both hydrogen and covalent bonds (Figure 14(a)). In their study, $Ti_3C_2T_x$ MXene flakes were synthesized by selectively etching the aluminum layer from the Ti_3AlC_2 MAX phase. The resulting flakes were analyzed using XRD, SEM, and AFM. To examine the impact of hydrogen bonding, the team fabricated four hydrogen-bonded MXene (HBM) films with varying sodium carboxymethyl cellulose (CMC) concentrations. They observed that the highest tensile strength was achieved at a CMC content of 10 wt%. Using this optimal concentration, they developed four sequentially bridged MXene (SBM) films (SBM-i to SBM-iv), each with an increasing boron content while keeping the CMC content fixed at 10 wt%. For comparative analysis, covalently bridged MXene (CBM) films were also synthesized using an identical sequence of immersion, rinsing, and

annealing steps. This systematic comparison allowed for a comprehensive evaluation of the mechanical properties and structural enhancements provided by the different bonding strategies.

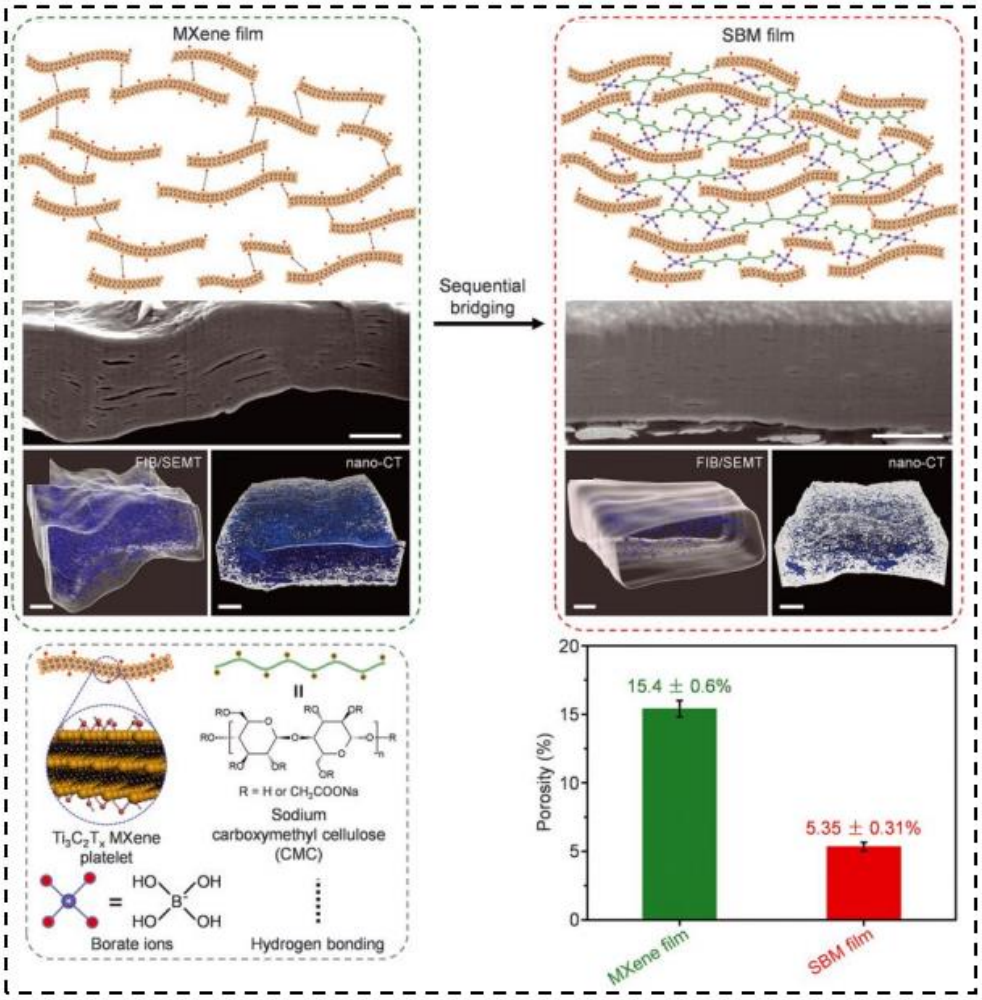

Figure 11. Hydrogen bond and covalent bond co-modification of MXene regulating interlayer spacing. Reprinted with permission [112]. Copyright 2022 Elsevier.

5.2.5. Other types of cross-linking

In addition to hydrogen bonding, ionic bonding, and covalent bonding, our team also structurally cross-linked sepiolite and MXene [114]. It was found that compared with pure MXene membranes, after excessive Sep was added to MXene nanosheets, the water flux of the Sep@MXene/CA composite membrane first increased and then decreased.

The incorporation of low concentrations of Sep into the MXene separation layer effectively increases the interlayer spacing, which broadens the mass transfer channels and improves the permeability of the resulting MXene-based composite membrane. Sep, a naturally hydrophilic inorganic material rich in silanol groups and hydroxyl bonds, promotes the swift penetration of water molecules, thereby enhancing the membrane's permeation flux. Remarkably, the addition of 10 mg of Sep nanomaterials increased the water flux of the composite membrane to 820.3 L $m^2 \cdot h^{-1} \cdot bar^{-1}$, representing a 30% improvement compared to the pure MXene membrane. However, it is well understood that membrane thickness directly impacts the resistance during the permeation process. Consequently,

excessive Sep addition disrupted the interlayer mass transfer channels of the MXene structure and increased the composite membrane's overall permeation resistance, resulting in a slight reduction in permeation flux.

5.3. Nanomaterial composites

The composite of MXene with graphene oxide (GO), layered double hydroxide (LDH), carbon nanotubes (CNT) and covalent organic framework (COF) can effectively regulate the interlayer spacing between MXene nanosheets and optimize their structure and performance. GO has abundant oxygen functional groups and high specific surface area. After composite with MXene, the interlayer spacing is increased through physical filling and chemical bonding, which improves the dispersion and mechanical strength of the material. The layered structure and ion exchange properties of LDH enable it to regulate the interlayer spacing through intercalation when composited with MXene, thereby enhancing the energy storage and catalytic performance. With its one-dimensional nanostructure and excellent conductive properties, carbon nanotubes can form conductive networks and support structures between layers when composited with MXene, increasing the interlayer spacing while improving the conductivity and mechanical strength. Covalent organic framework (COF) has a highly ordered pore structure and adjustable chemical functions. By composite with MXene, a stable organic network can be formed between layers, significantly regulating the interlayer distance and improving the chemical stability of the composite material. These composite strategies effectively regulate the interlayer spacing of MXene nanosheets through different mechanisms, thereby significantly improving their performance in different application scenarios.

5.3.1. Graphene oxide

Composites of graphene and MXene can also effectively control the interlayer spacing between MXene nanosheets. This composite structure can increase the interlayer spacing by introducing graphene nanosheets between MXene layers, thereby improving the conductivity and ion transport capacity of the material, which is of great significance in energy storage and other applications.

Yan *et al.* [115] assembled MXene nanosheets and rGO nanosheets by electrostatic self-assembly technology through the interaction between opposite charges (as shown in Figure 12(a)). This strong electrostatic interaction prevents MXene and rGO nanosheets from agglomerating and self-stacking. Then, the mixed suspension was processed using vacuum filtration to produce a flexible MXene/rGO composite film (as shown in Figure 12(b)). As shown in Figure 12(f), the XRD analysis of the pure MXene and MXene/rGO suspensions indicated that the interlayer spacing of pure MXene suspension was 1.31 nm, which is the typical diffraction peak of Ti3C2Tx-MXene nanosheets in water [116]. With the increase of rGO addition, the characteristic diffraction peak of MXene/rGO suspension shifted to 5.2°, indicating that the interlayer spacing increased to 1.67 nm, which indicates that rGO nanosheets are intertwined with MXene nanosheets [117]. In addition, it can be seen that when the rGO content increases from 5% to 10%, the height of the characteristic peak decreases, indicating that the stacking order decreases due to the hybridization of MXene and rGO. Nevertheless, the MXene/rGO composites were found to effectively alleviate the self-stacking tendency of rGO and MXene(as shown in Figure 12(c, d, e)), with the rGO nanosheets inserted between the MXene layers acting as conductive spacers,

increasing the interlayer spacing and providing unimpeded pathways for electrolyte ions, thereby ensuring high-rate performance.

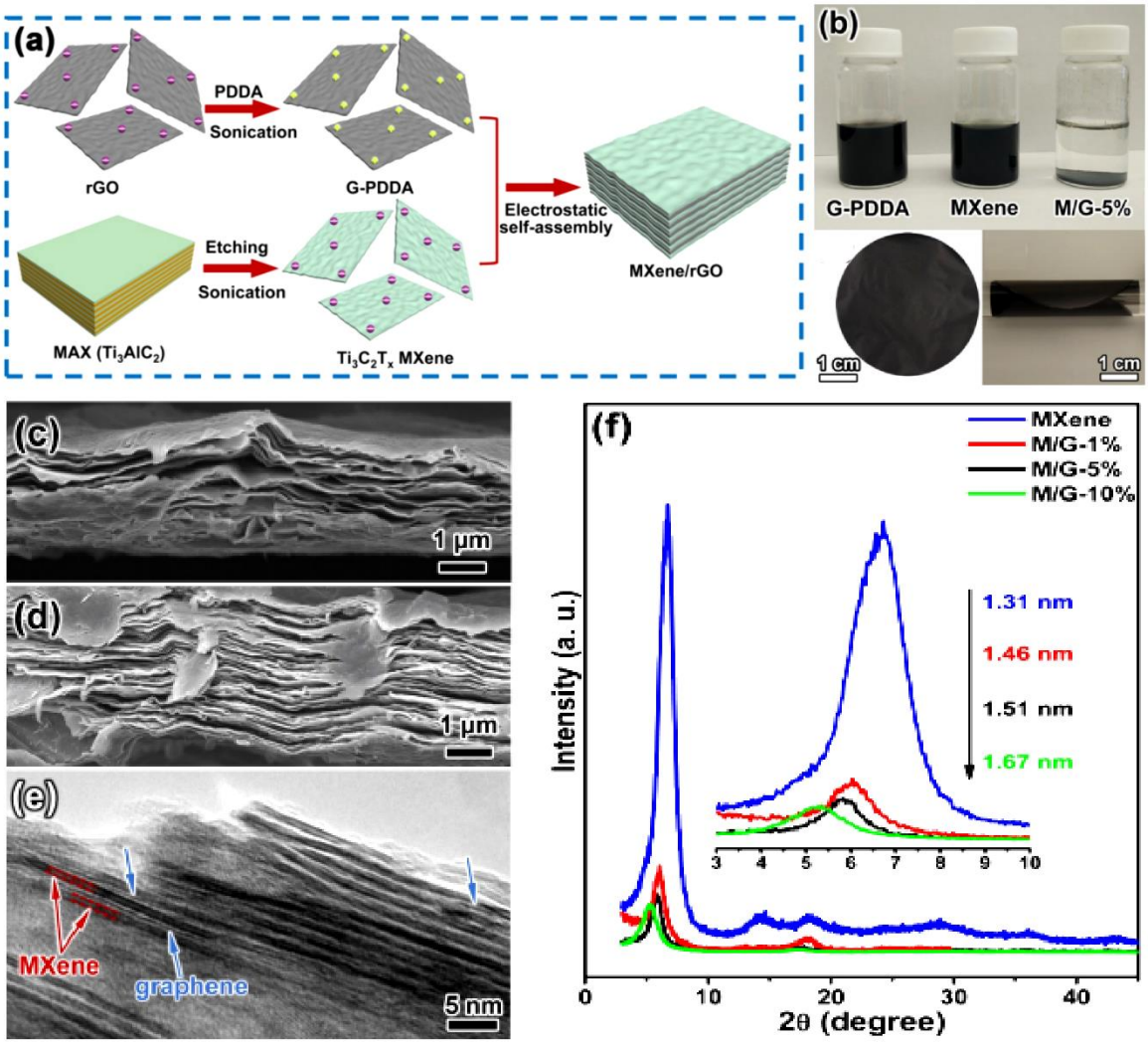

Figure 12. (a) Schematic illustration for the synthesis of the MXene/rGO hybrids. **(b)** Digital photographs of G-PDDA, MXene suspension, and M/G-5% hybrid; Digital photographs showing flexible, free-standing MXene/rGO hybrid films (M/G-5%). **(c, d)** cross-sectional SEM images of the pure MXene (c) and M/G-5% hybrid (d), insets are higher magnification SEM images. **(e)** TEM images of the M/G-5% hybrid. **(f)** XRD patterns of the prepared MXene and MXene/rGO hybrids. Reprinted with permission [115]. Copyright 2017 Wiley.

Yang *et al.* [118] introduced an efficient and rapid self-assembly method for fabricating three-dimensional porous antioxidant MXene/graphene (PMG) composites, utilizing an in-situ sacrificial metal zinc template to prevent the oxidation and self-stacking of MXene (as shown in Figure 13(A, B, C)). The study found that the PMG-5 composite retains a two-dimensional layered structure, but its surface is notably more wrinkled compared to the smooth and flat surface of pure MXene nanosheets. High-resolution transmission electron microscopy (HRTEM) identified a lattice fringe spacing of 1.39 nm between the layers, corresponding to the (002) crystal plane of MXene (as shown in Figure 13(D–G)). This spacing is slightly larger than the 1.30 nm observed in densely packed MXene. Additionally, lattice fringes with an interlayer spacing of 0.35 nm were attributed to the (002) crystal plane of reduced

graphene oxide (rGO). Importantly, the HRTEM images also showed that a single graphene layer is embedded within the MXene layers, forming a sandwich-like structure with an interlayer spacing of 1.71 nm. The observed spacing closely matches the combined interlayer distances of MXene and rGO, indicating a molecular-scale heterogeneous assembly of their nanosheets. This unique heterostructure prevents the direct stacking of MXene layers, allowing increased exposure of electroactive sites to electrolyte ions, thereby improving the composite's electrochemical performance.

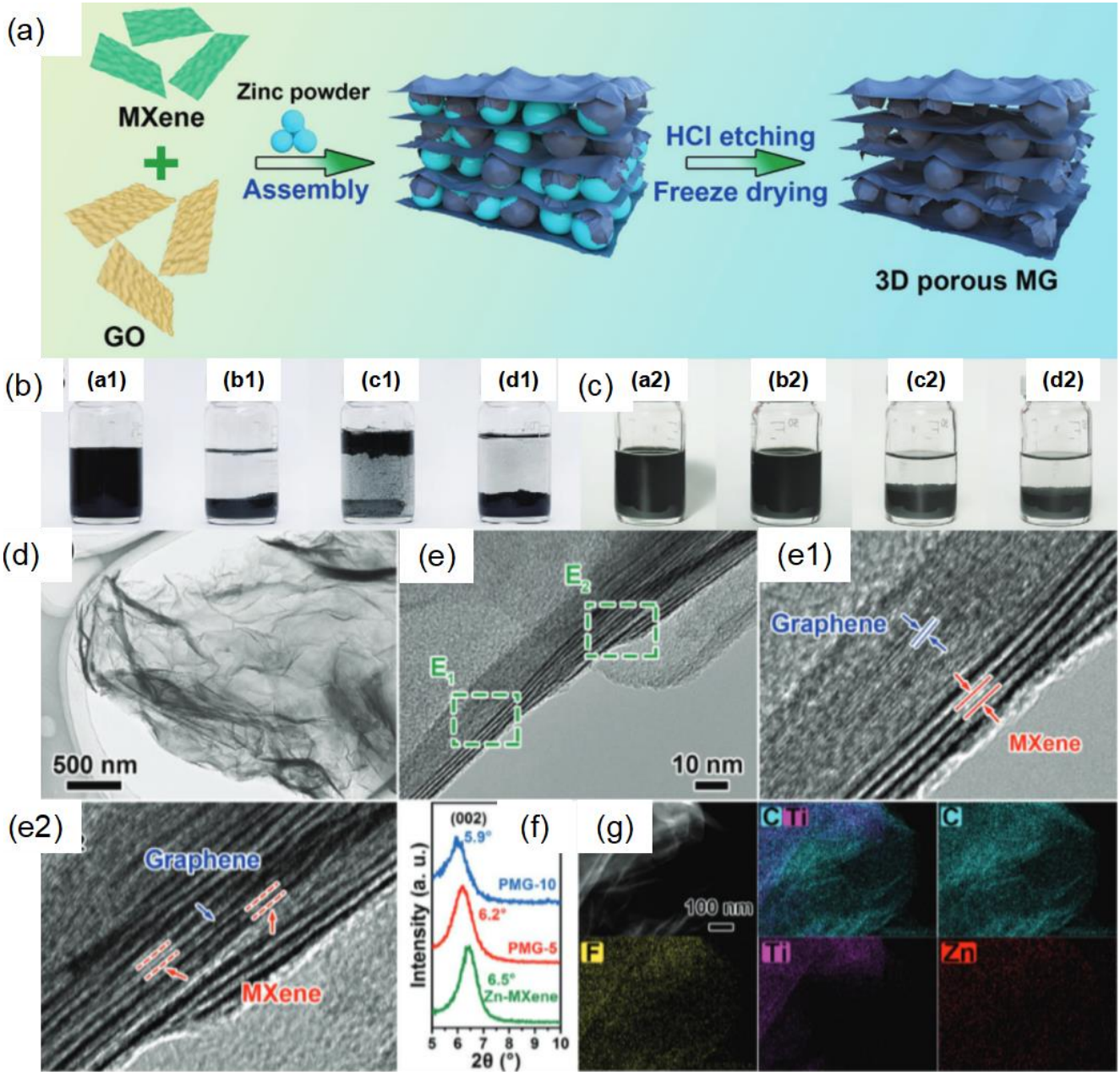

Figure 13. Schematic illustration and optical images. **(a)** Schematic illustration of the synthesis of 3D porous MG nanocomposite. **(b)** Optical imagesduring the synthesis process: (a1) MXene/GO colloidal suspension; (b1) after the addition of zinc powder and violently shaking; (c1) hydrochloric acid wasadded to remove the excess zinc powder; and (d1) complete removal of zinc powder. **(c)** Optical image of the MXene/GO (30 mg, 95:5 in weight) colloidalsuspension with different amounts of added zinc powder: (a2) 0 mg, (b) 100 mg, (c2) 200 mg, and (d2) 300 mg.

(d,e) TEM images. **(f)** XRD patterns of the Zn-MXene, PMG-5, and PMG-10 samples. **(g)** EDX elemental mapping images. Reproduced from ref. **Error! Reference source not found.** with the p ermission of Wiley.

5.3.2. Layered double hydroxide, LDH

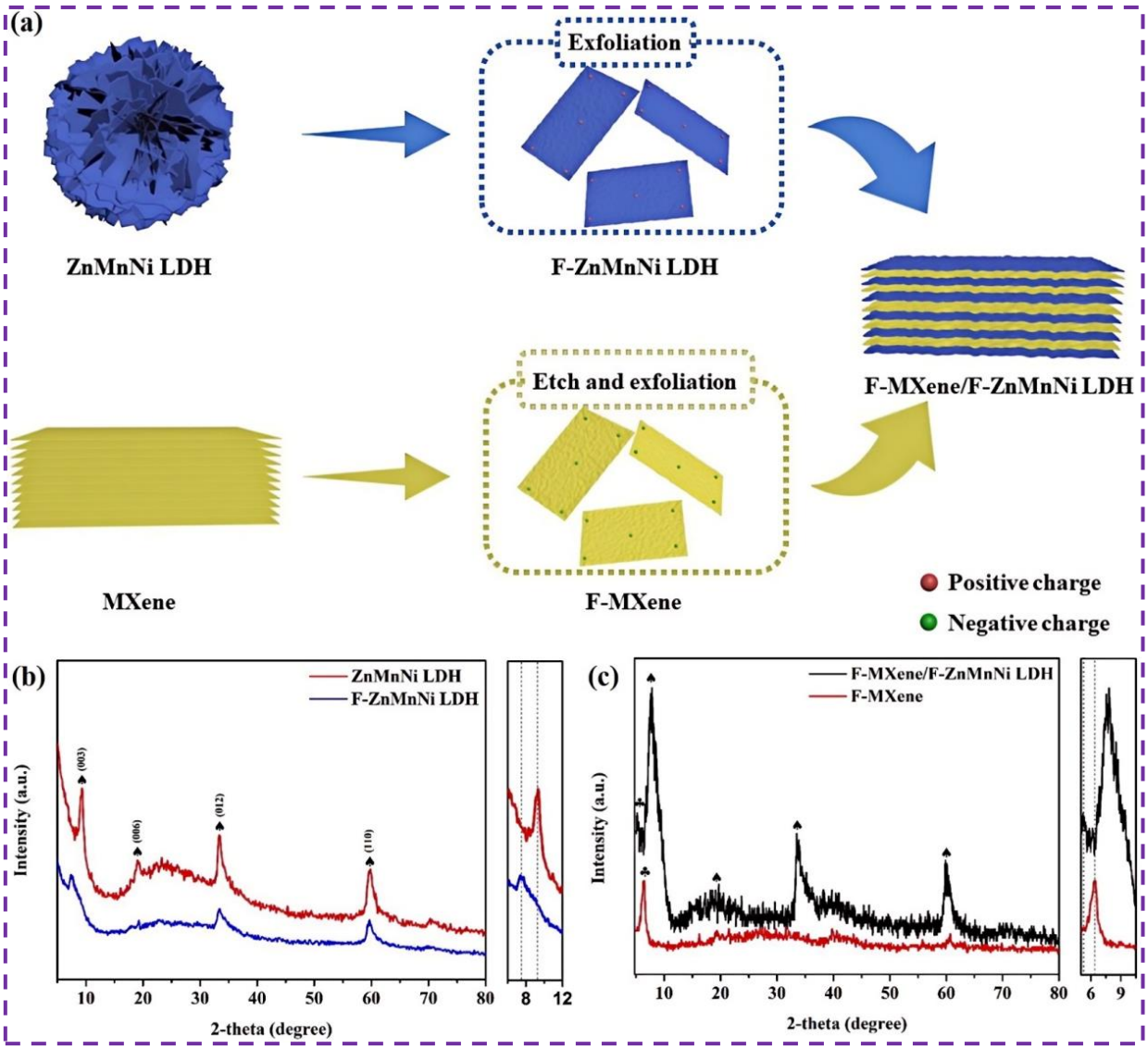

Figure 14. (a) Schematic illustration of the self-assembly process of the F-MXene/F-ZnMnNi LDH through electrostatic interaction. **(b)** XRD patterns of ZnMnNi LDH and F-ZnMnNi LDH. **(c)** XRD patterns of F-MXene and F-MXene/F-ZnMnNi LDH. Reprinted with permission [119]. Copyright 2020 ACS Publications.

Sun *et al.* [119] successfully fabricated a van der Waals heterostructure composed of exfoliated two-dimensional (2D) MXene (F-MXene) and exfoliated F-ZnMnNiLDH nanosheets. This structure was formed through electrostatic self-assembly, combining the negatively charged titanium carbide F-MXene nanosheets with positively charged F-ZnMnNiLDH nanosheets (Figure 14(a)). The prepared 2D/2D van der Waals heterostructure combines the excellent electronic conductivity, stable structure and excellent redox activity of F-MXene and F-ZnMnNiLDH. In the X-ray diffraction (XRD) pattern, a

prominent peak at 6.4° is observed for the (002) plane of F-MXene (Figure 14(b,c)), indicating the material's crystalline nature. However, after the etching and exfoliation process, the crystallinity of the F-MXene nanosheets decreases. The XRD spectrum of the FMXene/F-ZnMnNiLDH composite reveals that while the F-MXene retains its distinct (002) peak, the F-ZnMnNiLDH component exhibits nearly all of its characteristic peaks. Notably, the full width at half maximum (FWHM) of the (006) diffraction peak for F-ZnMnNiLDH in the composite is noticeably broader than that of pure F-ZnMnNiLDH, suggesting structural alterations in the F-ZnMnNiLDH nanosheets after self-assembly with F-MXene. Using the Bragg equation, the (001) plane exhibits a basal spacing of approximately 1.7 nm at 5°, aligning closely with previously reported values. Microscopic analysis further indicates that the F-MXene/F-ZnMnNiLDH composite forms a van der Waals heterostructure. The leftward shift of the (002) peak is ascribed to the orderly two-dimensional stacking of F-MXene and F-ZnMnNiLDH, resulting in an increased interlayer spacing. This increased spacing is beneficial for the transport and diffusion of electrolyte ions within the composite. Additionally, the lack of a TiO_2 peak in the diffraction pattern confirms that F-MXene remained unoxidized throughout the synthesis process.

5.3.3. Carbon nanotubes

Ajibade *et al.* [120] investigated the modification of polyacrylonitrile (PAN) ultrafiltration membranes using 3D nanocomposites of MXene and oxidized multi-walled carbon nanotubes (O-MWCNT) (as shown in Figure 15(a)). The study focused on investigating how varying MXene-to-O-MWCNT ratios in composite membranes influence their permeability, antifouling performance, and effectiveness in removing lubricating oil and soluble anionic and cationic dyes. The findings revealed that the introduction of MXene nanosheets significantly enhanced the membrane's permeability. Specifically, the pure water flux of the modified membrane (M1) improved from 190 L m-2 h-1 to 246 L m-2 h-1, while the oil-water separation flux increased from 76 L m-2 h-1 to 94 L m-2 h-1(as shown in Figure 15(d, e)). Further improvements in flux were observed when O-MWCNTs were added at a 3:1 ratio with MXene (M2). Although the membrane composed exclusively of O-MWCNTs (M3, 0:4) exhibited the highest permeability in terms of both pure water flux and oil-water separation, it had a lower oil rejection rate compared to membrane M4 (1:3), which provided a better balance between flux and rejection rate. The superior oil rejection capability of M4 was further supported by optical microscopy images and oil droplet distribution curves, which showed a significant reduction in oil droplet size from 100–900 nm to less than 5 nm after separation. This high oil rejection efficiency is attributed to the synergistic effects of the hydrophilicity and oil absorption properties of both MXene and O-MWCNT in the membrane's skin layer (as shown in Figure 15(f, g)). The slightly lower flux observed in membrane M1 (4:0) compared to M2 (3:1) and M4 (1:3) is likely due to the restacking of MXene nanosheets, which forms two-dimensional nanochannels within the composite membrane. The addition of O-MWCNTs significantly increases the spacing between MXene nanosheets, facilitating easier water molecule transport in membranes M2, M4, and M5 (2:2), with M4 exhibiting the highest flux (as shown in Figure 15(b, c)). This enhanced permeability in M4 is attributed to the larger interlayer spacing created by the higher concentrations of O-MWCNTs and MXene. Furthermore, the hydrophilic functional groups in O-MWCNTs promote the rapid movement of water molecules, further improving the membrane's overall permeability.

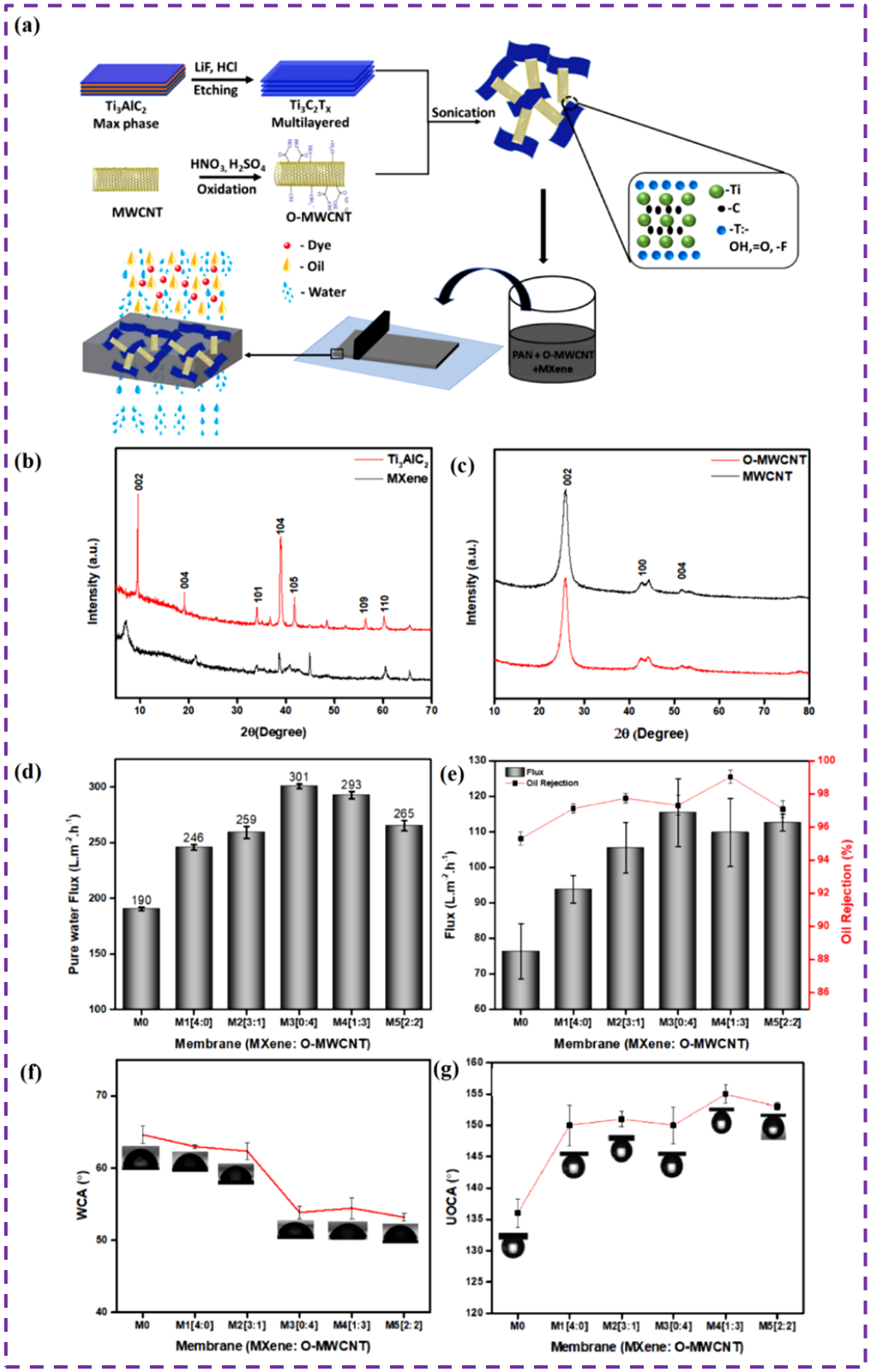

Figure 15. (a) Fabrication of MXene/O-MWCNT@PAN composite membrane for removal of complex oily waste emulsion. **(b,c)** XRD patterns for (b) Ti3AlC2 and MXene, and (c) MWCNT and O-MWCNT. **(d)** Pure water flux for M0-M5. **(e)** Flux and rejection for oil and water separation. (f) Water contact angle for membrane M0-M5. **(g)** Underwater oil contact angle for membrane M0-M5. Reprinted with permission [120]. Copyright 2021 Elsevier.

5.3.4. Covalent organic frameworks, COFs

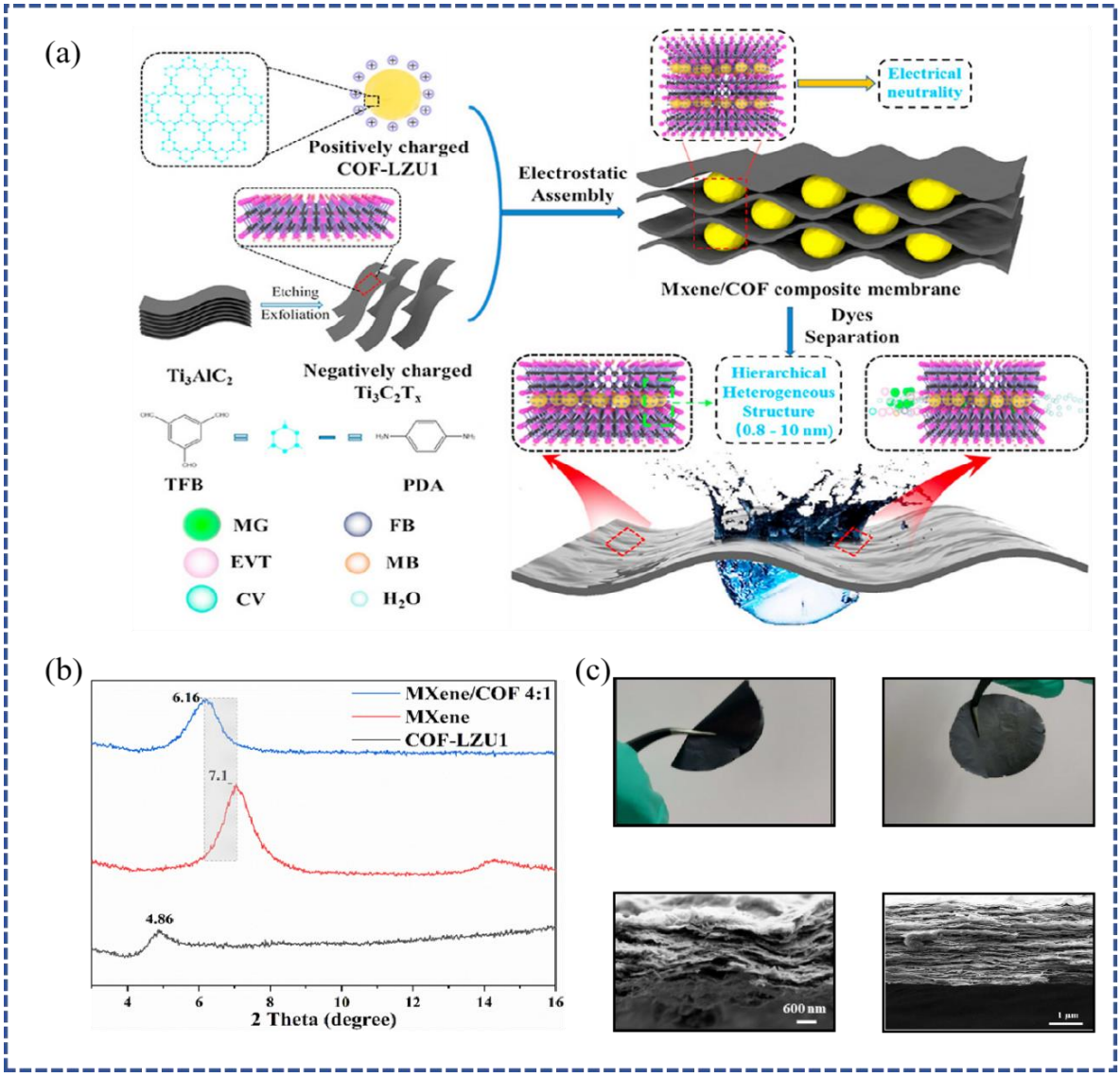

Figure 16. (a) Schematic demonstration the fabrication of MXene/COF composite membrane and its molecular sieving mechanism. **(b)** XRD patterns of COF-LZU1, Ti3C2Tx membrane and MXene/COF 4:1 composite membrane. **(c)** Digital photos of free-standing MXene/COF 4:1 composite membrane with folding and unfolding; SEM image of MXene/COF 4:1 composite membrane after long-time filtration experiment; The corresponding cross section. Reprinted with permission [121]. Copyright 2022 Elsevier.

Gong *et al.* [121] developed a multilayer porous MXene/COF composite membrane by electrostatically assembling MXene with COF-LZU1 (as shown in Figure 16(a)). In separation tests using five common dye solutions—methyl green (MG), ethyl violet (EVT), fuchsine (FB), crystal violet (CV), and methylene blue (MB)—the optimized MXene/COF 4:1 composite membrane exhibited exceptional water permeability, exceeding 169.3 L m-2 h-1 bar-1. As shown in Figure 16(b), X-ray diffraction (XRD) analysis verified the successful synthesis of COF-LZU1, with an average particle size of around 500 nm. The XRD data further indicated a shift in the (002) diffraction peak of the

MXene/COF composite membrane from 7.1° to 6.1°, suggesting that the addition of COF-LZU1 expanded the interlayer spacing of Ti3C2Tx from 1.27 nm to 1.45 nm. Furthermore, UV degradation experiments confirmed that the MXene/COF 4:1 composite membrane could be efficiently recycled under UV irradiation without experiencing any structural deterioration (as shown in Figure 16(c)). The membrane's exceptional dye separation performance is attributed to its layered heterogeneous structure, which features both micropores and mesopores, along with its robust photothermal conversion properties. This innovative membrane design offers significant potential for advancing both academic research and industrial applications in dye separation technologies.

5.3.5. MXene/g-C_3N_4

Wenyue *et al*. [122] developed a carbonized cellulose nanofiber/$Ti_3C_2T_x$ MXene/g-C_3N_4 heterojunction photocatalyst for the decomposition of contaminants (*e.g.*, methylene blue, rhodamine B, and tetracycline) upon visible light irradiation. The composite exhibits high photocatalytic efficiency due to its high surface area and excellent electron transport capacity.

The advantage of this composite is that the conductivity and structural stability of MXene combined with the visible light activity of g-C_3N_4 effectively promote the separation of photogenerated electron-hole pairs, thereby improving the photocatalytic performance. In addition, the addition of cellulose nanofibers further increased the specific surface area, improved the pore structure of the composites, and improved the performance of the materials in pollutant degradation.

5.4. Polymer composites

Combining MXene with polymers is a practical approach to adjusting the interlayer spacing of MXene nanosheets. By utilizing the diversity and adjustability of polymers, the structure and performance of composite materials can be optimized. Polymer chains can enter between MXene nanosheets through intercalation, increase the interlayer spacing, and improve the dispersion and mechanical properties of the material. At the same time, the long chain structure and flexible properties of the polymer can form a stable support network between the layers, improving the mechanical strength and flexibility of the composite material. In addition, the introduction of different functionalized polymers can give MXene composites specific chemical and physical properties, such as enhanced conductivity, improved chemical stability, and improved ion conductivity.

Conductive, flexible, and freestanding $Ti_3C_2T_x$/PDDA and $Ti_3C_2T_x$/PVA composites were fabricated using vacuum-assisted filtration (VAF) to create highly flexible $Ti_3C_2T_x$/PDDA and $Ti_3C_2T_x$/PVA films [114]. The zeta potential of the synthesized $Ti_3C_2T_x$ colloidal solution was recorded as −39.5 mV, confirming the negatively charged surface of $Ti_3C_2T_x$. This negative charge made the cationic polymer PDDA an ideal candidate for the fabrication of nanocomposites (Figure 17). The $Ti_3C_2T_x$/PDDA composite film produced via VAF exhibited an orderly stacking of layers throughout the film, as observed in Figure 17. The XRD pattern of the composite film showed a distinct peak at 4.7°, indicating that the $Ti_3C_2T_x$ flakes are orderly stacked along the [0001] direction. Notably, this peak appears at a lower angle compared to the pure $Ti_3C_2T_x$ film, which exhibited a peak at 6.5°. This shift in the peak position suggests that PDDA molecules intercalate between the $Ti_3C_2T_x$ flakes, resulting in a modified interlayer spacing.

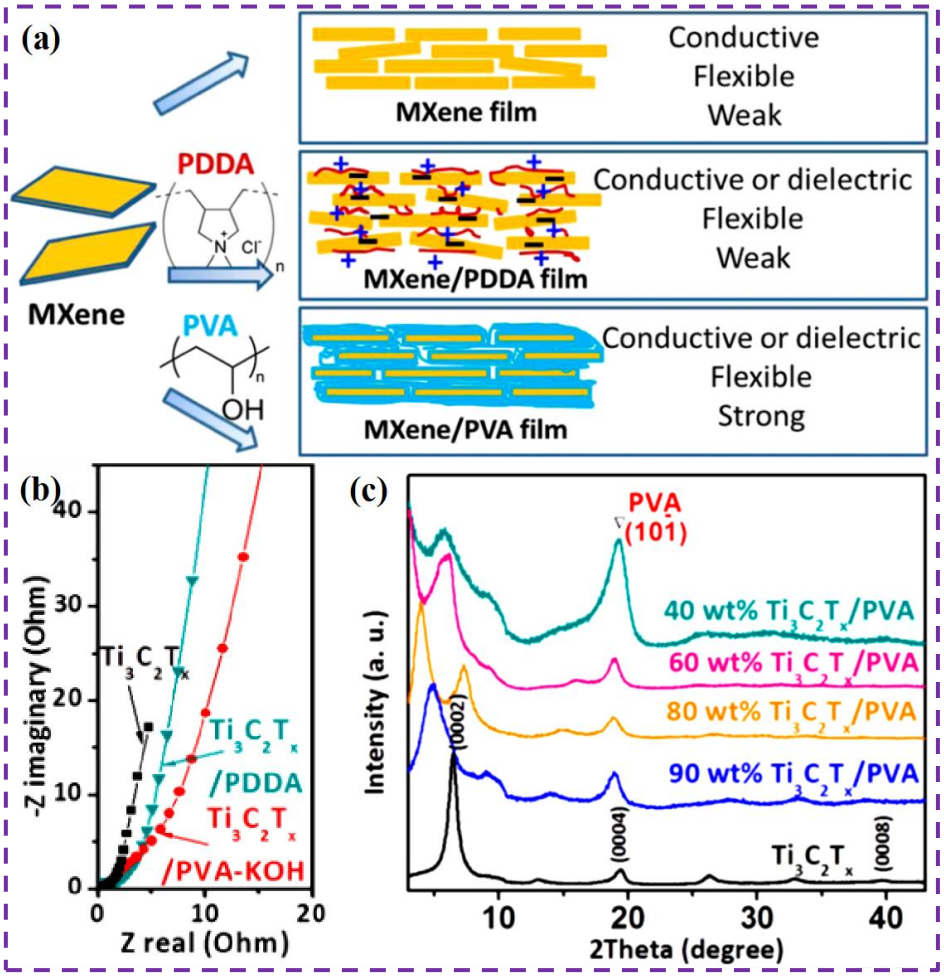

Figure 17. (a) A schematic illustration of MXene-based functional films with adjustable properties. **(b)** Nyquist plots for film electrodes. **(c)** XRD patterns of the Ti3C2Tx and Ti3C2Tx/PVA films. Reprinted with permission [114]. Copyright 2022 National Acad Sciences.

5.5. Neural networks

5.5.1. Prediction of MXene interlayer spacing control results by neural network

Artificial intelligence presents an efficient and precise approach for regulating the interlayer distance of MXene nanosheets by exploring and predicting optimal regulation strategies through a data-driven methodology. Neural networks, which are sophisticated computational models designed to simulate the information-processing capabilities of the human brain, are particularly adept at managing nonlinear and complex datasets. Through rigorous training, these networks can discern the intricate relationships between various input parameters (such as synthesis conditions and chemical modification methods) and output variables (such as MXene interlayer spacing and mechanical properties). As a result, neural networks are well-suited for the accurate prediction and design of MXene interlayer structures.

The principal advantage of AI-driven neural network models lies in their data-centric nature. By leveraging extensive experimental or simulation datasets, neural networks can autonomously uncover the underlying mechanisms and principles that govern the regulation of MXene interlayer spacing. By aggregating and integrating vast amounts of experimental data into a comprehensive database, neural

networks can efficiently screen thousands of potential condition combinations in a remarkably short period, thereby identifying the optimal regulation strategies. This capability significantly reduces the experimental cost and time traditionally required.

For example, Shariq *et al.* [123] employed this approach by embedding graphene nanosheets as nanofillers within the interlayer of MXene to mitigate aggregation and enhance the number of active sites, thereby promoting rapid ion exchange. Their research indicated that when the graphene nanosheet content was increased to 40%, the d-spacing of MXene expanded from 1.078 nm to 1.100 nm. The composite material was subsequently subjected to various electrochemical evaluations, including cyclic voltammetry (CV), galvanostatic charge-discharge (GCD), electrochemical impedance spectroscopy (EIS), and cycle stability tests. The experimental data obtained from these evaluations were then used to train several neural network models, including a Multiple Linear Regression (MLR) model, a Support Vector Regression (SVR) model, a Random Forest (RF) model, and an Artificial Neural Network (ANN) model. Among these models, the ANN demonstrated superior performance in predicting key performance indicators. A comparison of the predicted results with experimental data revealed that when the graphene nanosheet content was 20%, the performance indicators reached their optimal values. This study underscores the efficacy of neural networks in predicting and optimizing the composition and characteristics of different materials. In the context of MXene research, this AI-driven approach exhibits substantial potential for broad application. The initial successes documented in this study provide valuable insights for future research endeavors and highlight the significant promise of AI technology in advancing the field of MXene materials science.

5.5.2. Preparation of smart sensors using MXene with adjustable interlayer spacing

By regulating the interlayer spacing of MXene nanosheets, their performance in artificial intelligence applications can be significantly enhanced, particularly in areas such as data storage, neuromorphic computing, and smart sensors. Adjusting the interlayer spacing of MXene enables precise tuning of its electrical properties, thereby optimizing key aspects of data storage, including data writing and reading speeds, storage density, and energy efficiency. Additionally, the tunable interlayer spacing enables MXene to accurately mimic the signal transmission and processing of neurons. This optimization can enhance the conductivity and stability of MXene materials at low voltages, reducing energy consumption in neuromorphic computing—a critical factor for developing efficient biomimetic computing systems.
In the realm of smart sensors, MXene materials have gained popularity due to their high conductivity and environmental responsiveness. Utilizing diverse strategies to regulate interlayer spacing allows MXene materials to exhibit heightened sensitivity to various environmental conditions, such as gas, humidity, temperature, and pressure. This adaptability enables the creation of multifunctional integrated sensors capable of meeting AI systems' demands for complex environmental monitoring. For instance, Guo *et al.* [124] employed interlayer hydrogen bonds to combine Ti3C2Tx MXene with FPDMS sponge, resulting in an MFP sponge with high mechanical stability.

While MXene with adjustable interlayer spacing holds great promise in artificial intelligence, it also faces challenges, such as achieving precise interlayer distance control and maintaining long-term stability in complex environments. Future research should focus on exploring new regulation mechanisms and optimizing material preparation processes to fully harness the potential of MXene materials in AI hardware. Furthermore, interdisciplinary collaboration will be crucial for advancing the

application of MXene in AI, transitioning from basic material research to practical applications, and achieving further breakthroughs in artificial intelligence technology.

5.6. Chapter summary

This section examines various approaches to regulate the interlayer spacing of MXene membranes through surface functionalization, intercalation chemistry, composite with nanomaterials, composite with polymers, neural network prediction, *etc.*, and discusses the advantages and disadvantages of each method in detail. These methods have played an important role in optimizing the performance of MXene membranes and expanding their application areas.

The advantage of surface functionalization is that by changing the interaction forces between nanosheets, the interlayer spacing can be precisely adjusted, and the dispersion and stability of MXene can be improved. However, surface functionalization also has its disadvantages, that is, the original properties of MXene, such as conductivity and mechanical strength, may be changed in the process of introducing functional groups, so optimization and balance are required in the functionalization process. The advantage of intercalation chemistry is that it can significantly increase the interlayer spacing and improve the physical and chemical properties of the material. However, the disadvantage of intercalation chemistry is that the introduced intercalation agent may affect the purity and uniformity of the material, and the intercalation process is complicated and requires precise control of experimental conditions. The advantage of nanomaterial composites is that the interlayer spacing can be changed by introducing new interaction forces and new functions can be given to MXene. However, the disadvantage of this method is that the preparation process of the composite material is complicated, and the interaction between different nanomaterials needs to be carefully controlled to achieve the expected performance improvement. The advantage of polymer composites is that the polymer matrix can adjust the interlayer spacing of MXene through the action of molecular chains and significantly improve the mechanical properties, conductivity and thermal stability of the composite material. However, the disadvantage of this method is that the performance of the composite material is greatly affected by the type and distribution of the polymer, and the composite process requires optimization to guarantee the material's uniformity and stability. The advantage of neural network prediction is that it can quickly screen out the best control parameters, improve experimental efficiency, reduce the number of trial and error, and reduce costs. In addition, neural networks can discover patterns that are difficult to detect with traditional experimental methods, providing new ideas for material design. However, the disadvantage of neural network prediction is that it relies heavily on a large amount of high-quality data and advanced computing resources, and the training and optimization of the model requires interdisciplinary expertise and has a certain technical threshold.

In summary, through various strategies such as surface functionalization, intercalation chemistry, composite with nanomaterials, composite with polymers, and neural network prediction, the nanosheet spacing of MXene membranes can be effectively regulated and their performance can be optimized. These methods have their own advantages and disadvantages and are suitable for different application scenarios. By comprehensively applying these strategies, MXene membranes with excellent performance can be prepared, promoting their wide application in energy, environment, electronics, biomedicine and other fields.

6. Application of MXene material in AI field

This intersection between MXene materials and AI systems has opened novel avenues for the development of advanced hardware, data acquisition systems, and optimization processes. By leveraging AI-driven methodologies, researchers have not only enhanced MXene synthesis and functionality but also enabled innovative applications in neuromorphic computing, intelligent sensors, data storage, and flexible electronics.

6.1 AI-driven techniques in MXene research

The AI methodology has significantly advanced the discovery and optimization of MXene materials. A key application of AI in this regard is the use of machine learning algorithms to predict the structural and functional properties of MXene-based systems. For example, neural networks trained on an extensive dataset of MXene synthesis parameters have been used to identify optimal etching conditions that enable precise control of interlayer spacing and the distribution of functional groups. Building on this, Shrestha *et al.* [125] integrated machine intelligence and robotics to accelerate the design of programmable conductive mxenbased aerogels with customizable mechanical and electrical properties. A high-throughput platform has been developed by combining automated robotics with artificial intelligence and machine learning (AI/ML) technologies to optimize the fabrication of pairs of aerogels. The general process of the study was to synthesize 264 initial aerogels and then use an active learning cycle to produce 162 conductive aerogels. In this study, support vector machine (SVM) and artificial neural network (ANN), advanced big data computing tools, are used to predict and optimize key material properties. This innovative workflow enables bidirectional design capabilities: it allows accurate prediction of aerogel performance based on manufacturing parameters and facilitates reverse design to meet specific application requirements. The resulting aerogel exhibits outstanding properties, including high conductivity, pressure insensitivity, and customized compression elasticity, making it particularly suitable for applications such as wearable thermal management. The main contributions of this study include the seamless integration of machine intelligence to simplify material customization, the use of SHAP model interpretation to reveal complex structure-property relationships, and the establishment of a systematic framework for designing advanced nanomaterials. This scalable and adaptable approach not only advances aerogel research, but also has great potential in other areas, including haptic sensors and catalytic systems. By reducing the trial-and-error phase, these AI-driven approaches enable more efficient experimentation and resource utilization, paving the way for faster and more cost-effective material development.

AI has also been instrumental in facilitating the functionalization of MXenes for specific applications. High-throughput computational screening powered by AI models has identified new functional groups, such as chalcogens and halogens, that enhance MXene's electronic, catalytic, and mechanical properties. Experimental validation confirmed that these functionalizations significantly improved the performance of MXenes in neuromorphic devices and sensing applications.

6.2. MXene applications in neuromorphic computing

In the realm of neuromorphic computing, MXenes exhibit remarkable potential due to their exceptional electrical conductivity, mechanical stability, and tunable electronic properties. Artificial intelligence (AI) techniques have been instrumental in advancing the design of artificial synapses using MXene-based memristors, which replicate the plasticity of biological neural networks [126]. These devices are pivotal for the development of low-power, brain-inspired computing systems.

Separately, Yao *et al.* [127] developed an advanced electrochemical platform utilizing $BiFeO_3/Ti_3C_2$ MXene composites for the rapid and highly sensitive detection of Pb^{2+} ions in water. The composites, synthesized via a hydrothermal method, leverage their high conductivity and abundant surface active sites to significantly enhance electrochemical sensing performance. By integrating orthogonal experimental design with machine learning techniques such as back-propagation artificial neural networks (BPANN) and genetic algorithms (GA), the detection parameters were optimized to achieve a detection limit of 0.0001 μg/L, markedly surpassing traditional methods. Moreover, the platform demonstrated outstanding repeatability, stability, and anti-interference capability when tested with real lake water samples, achieving Pb2+ recovery rates between 98.79% and 101.3%. The study's key innovations include the application of machine learning for optimizing electrochemical sensor performance and significant enhancements in the conductivity and ion selectivity of composite materials. These advancements offer a novel framework for the rapid, portable, and efficient detection of heavy metal ions in environmental samples, addressing critical challenges in environmental monitoring and public health.

6.3. Intelligent Sensors for Real-Time AI Systems

MXene materials have redefined the capabilities of intelligent sensors, a cornerstone of AI systems. Their high surface area and conductivity make them highly sensitive to environmental stimuli. AI-enhanced designs have been utilized to improve sensor performance by predicting the interaction dynamics between MXene layers and target analytes. For instance, MXene-based gas sensors integrated with neural network models achieved higher accuracy and selectivity for multiple gas detection [128,129]. These sensors have applications in environmental monitoring, healthcare diagnostics, and industrial automation, providing real-time data for AI-driven decision-making.Recent advancements in AI-enabled sensor designs include MXene-based wearable devices that track physiological parameters such as heart rate, respiration, and joint movements [130]. These sensors have been embedded in smart textiles and coupled with AI algorithms for predictive health monitoring. For example, an AI model trained on sensor data successfully predicted early signs of cardiac anomalies, demonstrating the transformative potential of MXene-enabled wearable technology in personalized medicine [131,132].

6.4. Data storage and processing: A key AI enabler

The rapid growth of AI technologies demands efficient data storage and processing systems, and MXene materials are emerging as a solution [133]. Their high conductivity, layered structure, and stability make them suitable for energy storage devices such as supercapacitors and batteries, which are essential for powering AI hardware [134]. Beyond energy storage, MXenes have been integrated into non-volatile

memory devices, where their tunable resistive switching properties have enabled fast, reliable, and scalable data storage [135]. AI-driven optimization of these memory devices has improved their endurance and energy efficiency, paving the way for their adoption in edge computing systems.AI methodologies have also been applied to model the thermal and electrical properties of MXenes, ensuring their compatibility with existing semiconductor technologies [136]. This integration has enabled the development of AI processors with enhanced computational efficiency, particularly in resource-constrained environments.

6.5. Flexible electronics and AI-driven design

MXene materials' mechanical flexibility and lightweight nature make them ideal for flexible electronic devices, a growing focus in AI hardware. Transparent conductive films and flexible electrodes made from MXenes have been developed for foldable displays, wearable devices, and robotic systems [137]. AI-driven simulations have guided the design of these components, optimizing their performance under dynamic mechanical stress. For example, reinforcement learning models were used to design MXene-based electrodes for soft robotics, ensuring reliable performance under repetitive deformation [138].

6.6. Future Directions: AI-driven innovation in MXene research

Looking forward, the integration of AI and MXene materials offers immense potential for advancing both fields. Key future directions include:

(1) AI-Augmented Synthesis and Functionalization

AI techniques such as generative adversarial networks (GANs) and reinforcement learning can be employed to predict novel functionalizations and optimize synthesis routes. Real-time AI-driven monitoring systems could dynamically adjust synthesis parameters to produce MXenes with tailored properties, reducing material waste and production costs [139].

(2) High-Performance AI Hardware

MXenes' conductivity and tunability position them as ideal candidates for next-generation AI hardware [140]. Future research could focus on developing MXene-based components for brain-machine interfaces, autonomous systems, and quantum computing devices, all guided by AI-driven material design frameworks.

(3) Sustainable and Scalable Production

AI can address the scalability and sustainability challenges associated with MXene production by identifying eco-friendly etching agents and optimizing large-scale synthesis processes [141]. These efforts are crucial for transitioning MXene materials from laboratory research to industrial applications.

(4) AI-Enhanced Applications

Emerging applications, such as AI-driven smart cities and adaptive sensing networks, can benefit from MXene's multifunctionality. For instance, MXene-enabled sensors integrated into AI platforms could enhance urban infrastructure monitoring, predictive maintenance, and environmental management [142].

(5) Cross-Disciplinary Collaboration

The convergence of AI and MXene research requires interdisciplinary collaboration between materials scientists, computer engineers, and AI researchers [143]. Joint efforts in this area could yield groundbreaking advancements in intelligent systems, energy-efficient hardware, and sustainable technologies.

6.7. Chapter Summary

MXene materials are redefining the boundaries of what is possible in AI applications. Their unique properties, combined with AI-driven optimization techniques, have enabled significant advancements in neuromorphic computing, intelligent sensors, data storage, and flexible electronics. The use of AI in material design and functionalization has not only accelerated research but also opened new possibilities for future technologies. By addressing current challenges in scalability and compatibility, MXene materials, guided by AI methodologies, are poised to play a central role in shaping the future of intelligent systems. This synergy between AI and MXene materials represents a promising pathway toward more efficient, adaptive, and sustainable technologies.

7. Conclusion

Starting from the research on two-dimensional material anion exchange membranes, this paper emphasizes the development of MXene-based anion exchange membranes and explores their potential applications in this domain. First, the preparation methods of MXene are reviewed in detail, and high-quality MXene nanosheets are obtained by hydrofluoric acid preparation, electrochemical etching, hydrothermal synthesis, and artificial intelligence-assisted preparation. Then, the preparation process of MXene membranes is introduced, such as vacuum filtration, casting, electrospinning, and artificial intelligence neural network techniques to prepare MXene films, aiming to form uniform and stable MXene membranes. Furthermore, this paper examines the mechanism by which interlayer spacing regulation impacts the performance of ion exchange membranes, highlighting its crucial role in enhancing ion conduction, mechanical strength, and chemical stability. In order to optimize the performance of MXene membranes, this paper explores a variety of strategies for regulating the interlayer spacing of MXene nanosheets, including surface functionalization, intercalation chemistry, composite with nanomaterials, composite with polymers, neural network prediction, and other methods.

At the same time, in the research on regulating the interlayer spacing of MXene exchange membranes, the following major challenges are faced: MXene materials are easily oxidized and degraded in air and water, which poses a challenge to their long-term stability in practical applications. In order to improve the stability of the material, effective protection measures and surface modification technologies must be developed to prevent the oxidation and degradation of MXene materials. In addition, the preparation process of MXene materials involves multi-step chemical reactions and high-purity reagents, resulting in high costs. To make MXene exchange membranes competitive in commercial applications, more economical and efficient preparation methods must be developed to reduce production costs. In large-scale production, the consistency and quality control of materials must also be addressed. Precise regulation of the interlayer spacing of MXene nanosheets directly affects the performance of the membrane. It is necessary to conduct in-depth research on the mechanisms and effects of different regulation methods to achieve precise control of the interlayer spacing. At the same time, new regulation technologies need to be developed to further improve the performance and application range of the membrane. In addition to the regulation of interlayer spacing, it is also necessary to comprehensively consider the mechanical strength, ion selectivity, conductivity and chemical stability of the membrane. There is often a trade-off between these properties, and it is necessary to achieve the optimal balance of comprehensive performance through optimized design and the introduction of multi-composite

materials. By addressing these challenges, MXene exchange membranes are expected to play a more important role in energy storage, separation, catalysis and other fields, and promote the development and application of related technologies. In addition, there are still some limitations in this paper that require further investigation. A major problem is the versatility of AI models; These models often rely on high-quality datasets, and their predictions can be difficult to adapt to different synthetic environments. In addition, achieving consistent layer spacing can still be challenging, especially when scaling up production, where small variations in process conditions can lead to inconsistencies in the structural and functional properties of the MXene. Addressing these challenges will provide a more balanced perspective and provide a roadmap for future research to further refine AI models and develop standardized protocols for MXene membrane fabrication.

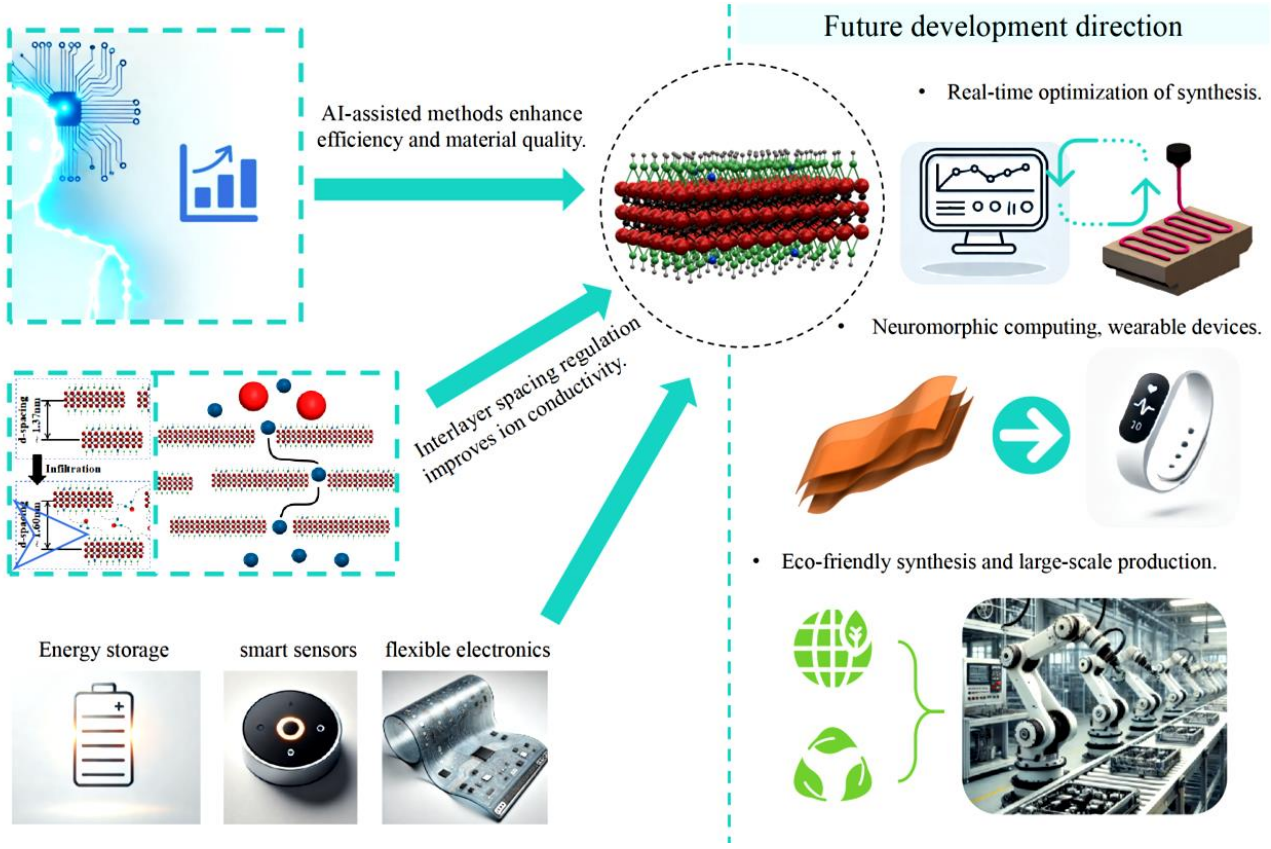

Figure 18. Synthesis of MXene research outcomes and future directions.

In future research, several important directions for regulating the interlayer spacing of MXene exchange membranes deserve special attention. First, one of the keys is the development of new control technologies, including smart response materials that can dynamically respond to external stimuli such as temperature, pH and light to precisely control the interlayer spacing; nano-scale mechanical control, using nanomechanical technology to precisely control the interlayer spacing of MXene nanosheets; and advanced chemical modification methods, which precisely control the interlayer spacing through molecular design and chemical reactions. Secondly, a key focus area is the development of multifunctional composite materials, incorporating components like GO, LDH, CNT, and COF, to enhance the functionality and optimize the performance of MXene-based exchange membranes; the development of new polymer composites to improve the mechanical strength, chemical stability and ion

conductivity of the membrane; and the exploration of the potential of MXene and a variety of materials to form multifunctional composite membranes. In addition, key research on the prospects for the industrial application of MXene exchange membranes is also crucial, including the development of large-scale production technologies, improving the economic efficiency of MXene preparation and membrane preparation, reducing production costs, and ensuring the consistency and quality control level of the membrane; conducting long-term stability evaluations to verify its durability and reliability in practical applications; and exploring its wide application in water treatment, gas separation, electrochemical energy storage and catalysis. Finally, prioritizing environmental sustainability and eco-friendliness should also serve as a key focus for future research endeavors, including the advancement of environmentally friendly MXene synthesis and membrane preparation methods, reducing the use of harmful chemicals and waste generation; research on degradable or recyclable MXene composite materials, promoting recycling and environmental protection. Through continuous research and innovation in these directions, MXene exchange membranes are expected to play an important role in future scientific and industrial applications and promote progress in related fields.

In general, the precise control of MXene interlayer spacing provides new approaches and ideas for the development of high-performance AEMs, provides a systematic research idea and technical route for the future application of MXene materials in high-performance anion exchange membranes, and looks forward to its broad application prospects in energy storage, catalysis, separation and other fields.

Acknowledgments

The authors acknowledge the National Natural Science Foundations of China (Grant Nos. 52250005, 21875271, U20B2021, 21707147, 51372046, 51479037, 91226202, and 91426304), the National Key Research and Development Program of China (No. 2024YFB3817300), the support of the Key R & D Projects of Zhejiang Province (No. 2022C01236, 2019C01060), the Entrepreneuship Program of Foshan National Hi-tech Industrial Development Zone, the Major Project of the Ministry of Science and Technology of China (Grant No. 2015ZX06004-001), Ningbo Natural Science Foundations (Grant Nos. 2014A610006, 2016A610273, and 2019A610106), The Project of Civil Aircraft Fire Science and Safety Engineering Key Laboratory of Sichuan Province (MZ2023JB03) and The Project of Civil Aviation Flight University of China (PHD2023-066) and Key Research and Development Program of Sichuan Province (2024YFHZ0039).

Authors' contribution

Conceptualization, Shiyu Du and Kexin Lv; methodology, Hengcheng Wan; software, Chenchen Qi; validation, Wenwei Wang; formal analysis; investigation, Kexin Lv; resources, Xiang Liu, Hongsen Wei; data curation, Hongjie Zhu; writing—original draft preparation, Kexin Lv; writing—review and editing, Shiyu Du and Hengcheng Wan; visualization, Lei Zhang; supervision, Yumo Wang.; project administration, Juhong Yu; funding acquisition, Shiyu Du. All authors have read and agreed to the published version of the manuscript.

Conflicts of interests

We declare that we have no financial and personal relationships with other people or organizations that can inappropriately influence our work, there is no professional or other personal interest of any nature or kind in any product, service and company that could be construed as influencing the manuscript.

References

[1] Aarhaug TA, Kjos OS, Ferber A, Hsu JP, Bacquart T. Mapping of hydrogen fuel quality in europe. *Front. Energy Res.* 2020, 8.
[2] Salam MA, Ahmed K, Akter N, Hossain T, Abdullah B. A review of hydrogen production via biomass gasification and its prospect in Bangladesh. *Int. J. Hydrogen Energy* 2018, 43(32):14944–14973.
[3] Eikeng E, Makhsoos A, Pollet BG. Critical and strategic raw materials for electrolysers, fuel cells, metal hydrides and hydrogen separation technologies. *Int. J. Hydrogen Energy* 2024, 71:433–464.
[4] Hora C, Dan F, Rancov N, Badea GE, Secui C. Main trends and research directions in hydrogen generation using low temperature electrolysis: A systematic literature review. *Energies* 2022, 15(16):6076.
[5] Amikam G, Nativ P, Gendel Y. Chlorine-free alkaline seawater electrolysis for hydrogen production. *Int. J. Hydrogen Energy* 2018, 43(13):6504–6514.
[6] Aldakheel F, Kandekar C, Bensmann B, Dal H, Hanke-Rauschenbach R. Electro-chemo-mechanical induced fracture modeling in proton exchange membrane water electrolysis for sustainable hydrogen production. *Comput. Methods Appl. Mech. Eng.* 2022, 400:115580.
[7] Vincent I, Kruger A, Bessarabov D. Hydrogen production by water electrolysis with an ultrathin anion-exchange membrane (AEM). *Int. J. Electrochem. Sci.* 2018, 13(12):11347–11358.
[8] Lahrichi A, El Issmaeli Y, Kalanur SS, Pollet BG. Advancements, strategies, and prospects of solid oxide electrolysis cells (SOECs): Towards enhanced performance and large-scale sustainable hydrogen production. *J. Energy Chem.* 2024, 94:688–715.
[9] Miller HA. Green hydrogen from anion exchange membrane water electrolysis. *Curr. Opin. Electrochem.* 2022, 36:101122.
[10] Kang SY, Park JE, Jang GY, Kim O-H, Kwon OJ, *et al*. High-performance and durable water electrolysis using a highly conductive and stable anion-exchange membrane. *Int. J. Hydrogen Energy* 2022, 47(15):9115–9126.
[11] Lei J, Liu X, Chen X, Guan P, Feng W, *et al*. Multi-length-scale heterogeneous structured ion exchange membranes for cost-effective electrolysis and hydrogen production. *Chem. Eng. J.* 2022, 431:133994.
[12] Fischer L, Hartmann SS, Maljusch A, Däschlein C, Prymak O, *et al*. The influence of anion-exchange membrane nanostructure onto ion transport: Adjusting membrane performance through fabrication conditions. *J. Membr. Sci.* 2023, 669:121306.
[13] Xu W, Wang W, Zhang X, Wang M, Wang Q, *et al*. Study on the adsorption rate of anion exchange absorbents for capturing carbon dioxide in ambient air. *Chem. Eng. Res. Des.* 2024, 201:503–509.
[14] Schropp E, Campos-Carriedo F, Iribarren D, Naumann G, Bernäcker C, *et al*. Environmental and material criticality assessment of hydrogen production via anion exchange membrane electrolysis. *Appl. Energy* 2024, 356:122247.
[15] Wan L, Xu Z, Xu Q, Pang M, Lin D, *et al*. Key components and design strategy of the membrane electrode assembly for alkaline water electrolysis. *Energy Environ. Sci.* 2023, 16(4):1384–1430.
[16] Simari C, Caprì A, Ur Rehman MH, Enotiadis A, Gatto I, *et al.* Composite anion exchange membranes based on polysulfone and silica nanoscale ionic materials for water electrolyzers. *Electrochim. Acta* 2023, 462:142788.
[17] Zhou J, Chen J, Ding A, Nie Y, Li Z, *et al*. Synthesis and properties of novel crosslinking anion exchange membranes based on quaternary poly(fluorene-piperidine). *Colloid Interface Sci.*

Commun. 2022, 46:100584.
[18] Chu JY, Lee KH, Kim AR, Yoo DJ. Improved electrochemical performance of composite anion exchange membranes for fuel cells through cross linking of the polymer chain with functionalized graphene oxide. *J. Membr. Sci.* 2020, 611:118385.
[19] Zhang D, Xu S, Wan R, Yang Y, He R. Functionalized graphene oxide cross-linked poly(2,6-dimethyl-1,4-phenylene oxide)-based anion exchange membranes with superior ionic conductivity. *J. Power Sources* 2022, 517:230720.
[20] Ni J, Wang J, Zhao S, Zhong F, Qu T, *et al*. LDH nanosheets anchored on bacterial cellulose-based composite anion exchange membranes for significantly enhanced strength and ionic conductivity. *Appl. Clay Sci.* 2022, 217:106391.
[21] Zhang X, Yu Z, Tang J, Huang J, Tang X, *et al*. Mxenes as inorganic fillers for the construction of poly (aryl piperidinium) anion exchange membranes with microphase separation structures to enhance ionic conductivity. *Fuel* 2024, 365:131177.
[22] Naguib M, Kurtoglu M, Presser V, Lu J, Niu J, *et al*. Two-dimensional nanocrystals produced by exfoliation of Ti3AlC2. *Adv. Mater.* 2011, 23(37):4248–4253.
[23] Wei X, Xue K, Wei Y, Wang S, Zhang X, *et al*. Two-dimensional copper vanadate intercalated vanadium carbide MXene nanoplates as a high-performance cathode for aqueous Zn-ion batteries. *Synth. Met.* 2024, 305:117600.
[24] Zhu Z, Xia Q, Wang L, Hu Q, Chang Y, *et al*. In situ grown VO2/V2C MXene and its supercapacitor applications. *J. Energy Storage* 2024, 88:111484.
[25] Li S, Li Y, Yuan Z, Li J, Butenko D, *et al*. A novel MXene-bridged Z-scheme ZnO@Nb2CTx MXene@carbon nitride nanosheets photocatalyst for efficient enrofloxacin degradation. *Chem. Eng. J.* 2024, 489:151505.
[26] Liu L, Cui M, Ambuchi JJ, Niu S, Li X, *et al.* H*ads dynamics engineering via bimetallic Pd-Cu@MXene catalyst for enhanced electrocatalytic hydrodechlorination. *Environ. Res.* 2024, 252:118859.
[27] Wang D, Zhang D, Zhang H, Wang Z, Wang J, *et al*. Quantitative detection of multi-component chemical gas via MXene-based sensor array driven by triboelectric nanogenerators with CNN-GRU model. *Sens. Actuators, B* 2024, 417:136101.
[28] Zhu F, Tao J, Yan M, Huang S, Irshad MS, *et al*. NiS2-MoS2@MXene heterostructures for enhancing polysulfide adsorption and conversion of LiS battery. *Sustainable Mater.Technol.* 2024, 39:e00868.
[29] Li Z, Li Y, Zhao W, Feng Y, Zhou B, *et al*. Flexible, hierarchical MXene@SWNTs transparent conductive film with multi-source thermal response for electromagnetic interference shielding. *Compos. Sci. Technol.* 2024, 249:110484.
[30] Wu Z, Yang T, Xing Y, Huang P, Li B, *et al*. MXene/BC@CoFe2O4 aerogel with excellent electromagnetic interference shielding and enhanced mechanical property. *J. Alloys Compd.* 2024, 985:174117.
[31] Li W, Li Y, An L, Zou Z, Cong Z, *et al.* Synergistic MXene/NiCo2S4 composite for high-performance flexible all-solid-state supercapacitors. *J. Energy Storage* 2024, 93:112398.
[32] Long C, Lu C, Li Y, Wang Z, Zhu H. N-spirocyclic ammonium-functionalized graphene oxide-based anion exchange membrane for fuel cells. *Int. J. Hydrogen Energy* 2020, 45(38):19778–19790.
[33] Zafari M, Kikhavani T, Ashrafizadeh SN. Hybrid surface modification of an anion exchange membrane for selective separation of monovalent anions in the electrodialysis process. *J. Environ. Chem. Eng.* 2022, 10(1):107014.
[34] Liu X, Fu Q, Li Z, Wang H, Ren J. Modulating surface electron density of hydrophilic/high-conductive MXene/Ni(OH)2/NF heterostructures for efficient asymmetric supercapacitors. *Diamond Relat. Mater.* 2023, 140:110474.
[35] Sha W, Guo Y, Yuan Q, Tang S, Zhang X, *et al*. Artificial intelligence to power the future of materials science and engineering. *Adv. Intell. Syst.* 2020, 2(4):1900143.
[36] He M, Zhang L. Machine learning and symbolic regression investigation on stability of MXene materials. *Comput. Mater. Sci* 2021, 196:110578.
[37] Tian S, Zhou K, Huang C, Qian C, Gao Z, *et al.* Investigation and understanding of the

mechanical properties of MXene by high-throughput computations and interpretable machine learning. *Extreme Mech. Lett.* 2022, 57:101921.
[38] Marchwiany ME, Birowska M, Popielski M, Majewski JA, Jastrzębska AM. Surface-related features responsible for cytotoxic behavior of MXenes layered materials predicted with machine learning approach. *Materials* 2020, 13(14):3083.
[39] Rajan AC, Mishra A, Satsangi S, Vaish R, Mizuseki H, *et al.* Machine-learning-assisted accurate band gap predictions of functionalized MXene. *Chem. Mater.* 2018, 30(12):4031–4038.
[40] Rong C, Zhou L, Zhang B, Xuan F. Machine learning for mechanics prediction of 2D MXene-based aerogels. *Compos. Commun.* 2023, 38:101474.
[41] Frey NC, Wang J, Vega Bellido GI, Anasori B, Gogotsi Y, *et al*. Prediction of synthesis of 2D metal carbides and nitrides (MXenes) and their precursors with positive and unlabeled machine learning. *ACS Nano.* 2019, 13(3):3031–3041.
[42] Ma X, Lan C, Lin H, Peng Y, Li T, *et al.* Designing desalination MXene membranes by machine learning and global optimization algorithm. *J. Membr. Sci.* 2024, 702:122803.
[43] Hussain I, Sajjad U, Kewate OJ, Amara U, Bibi F, *et al*. Double transition-metal MXenes: Classification, properties, machine learning, artificial intelligence, and energy storage applications. *Mater. Today Phys.* 2024, 42:101382.
[44] Chaudhary V, Khanna V, Ahmed Awan HT, Singh K, Khalid M, *et al*. Towards hospital-on-chip supported by 2D MXenes-based 5th generation intelligent biosensors. *Biosens. Bioelectron.* 2023, 220:114847.
[45] Patel M, Hemanth NR, Gosai J, Mohili R, Solanki A, *et al*. MXenes: promising 2D memristor materials for neuromorphic computing components. *Trends Chem.* 2022, 4(9):835–849.
[46] Chen R, Jia X, Zhou H, Ren S, Han D, *et al*. Applications of MXenes in wearable sensing: Advances, challenges, and prospects. *Mater. Today* 2024, 75:359–385.
[47] Li R, Zhang L, Shi L, Wang P. MXene Ti3C2: An effective 2d light-to-heat conversion material. *ACS Nano* 2017, 11(4):3752–3759.
[48] Naguib M, Gogotsi Y, Barsoum MW. Mxenes: A new family of two-dimensional materials and its application as electrodes for Li and Na-Ion batteries. *ECS Meeting Abstracts* 2015, MA2015-01(9):849.
[49] Zhang X, Lei J, Wu D, Zhao X, Jing Y, *et al*. A Ti-anchored Ti2CO2 monolayer (MXene) as a single-atom catalyst for CO oxidation. *J. Mater. Chem. A* 2016, 4(13):4871–4876.
[50] Su D, Zhang H, Zhang J, Zhao Y. Design and synthesis strategy of mxenes-based anode materials for sodium-ion batteries and progress of first-principles research. *Molecules* 2023, 28(17):6292.
[51] Abid MZ, Rafiq K, Aslam A, Jin R, Hussain E. Scope, evaluation and current perspectives of MXene synthesis strategies for state of the art applications. *J. Mater. Chem. A* 2024, 12(13):7351–7395.
[52] Wang S, Liu Y, Liu Y, Hu W. Effect of HF etching on titanium carbide (Ti3C2Tx) microstructure and its capacitive properties. *Chem. Eng. J.* 2023, 452:139512.
[53] Ghidiu M, Lukatskaya MR, Zhao M, Gogotsi Y, Barsoum MW. Conductive two-dimensional titanium carbide 'clay' with high volumetric capacitance. *nature* 2014, 516(7529):78–81.
[54] Malaki M, Maleki A, Varma RS. MXenes and ultrasonication. *J. Mater. Chem. A* 2019, 7(18):10843–10857.
[55] Kotasthane V, Tan Z, Yun J, Pentzer EB, Lutkenhaus JL, *et al*. Selective etching of Ti3AlC2 MAX phases using quaternary ammonium fluorides directly yields Ti3C2Tz MXene nanosheets: Implications for energy storage. *ACS Appl. Nano Mater.* 2023, 6(2):1093–1105.
[56] Sheng X, Li S, Huang H, Zhao Y, Chen Y, *et al*. Anticorrosive and UV-blocking waterborne polyurethane composite coating containing novel two-dimensional Ti3C2 MXene nanosheets. *J. Mater. Sci.* 2021, 56(6):4212–4224.
[57] Halim J, Lukatskaya MR, Cook KM, Lu J, Smith CR, *et al.* Transparent conductive two-dimensional titanium carbide epitaxial thin films. *Chem. Mater.* 2014, 26(7):2374-2381.
[58] Yin T, Li Y, Wang R, Al-Hartomy OA, Al-Ghamdi A, *et al*. Synthesis of Ti3C2Fx MXene with controllable fluorination by electrochemical etching for lithium-ion batteries applications. *Ceram. Int.* 2021, 47(20):28642-28649.
[59] Yang S, Zhang P, Wang F, Ricciardulli AG, Lohe MR, *et al.* Fluoride-Free synthesis of two-dimensional

titanium carbide (MXene) using a binary aqueous system. *Angew. Chem. Int. Ed.* 2018, 57(47):15491–15495.
[60] Sun W, Shah SA, Chen Y, Tan Z, Gao H, *et al*. Electrochemical etching of Ti2AlC to Ti2CTx (MXene) in low-concentration hydrochloric acid solution. *J. Mater. Chem. A* 2017, 5(41):21663–21668.
[61] Pang S-Y, Wong Y-T, Yuan S, Liu Y, Tsang M-K, *et al.* Universal strategy for HF-Free facile and rapid synthesis of two-dimensional mxenes as multifunctional energy materials. *J. Am. Chem. Soc.* 2019, 141(24):9610–9616.
[62] He H, Wang J, Xia Q, Wang L, Hu Q, *et al*. Effect of electrolyte on supercapacitor performance of two-dimensional molybdenum carbide (Mo2CTx) MXene prepared by hydrothermal etching. *Appl. Surf. Sci.* 2021, 568:150971.
[63] Alhabeb M, Maleski K, Anasori B, Lelyukh P, Clark L, *et al*. Guidelines for synthesis and processing of two-dimensional titanium carbide (Ti3C2Tx MXene). *Chem. Mater.* 2017, 29(18):7633–7644.
[64] Diebler H. Stability and structure of complexes of transition metal ions with nucleotides and related compounds. *Inorg. Chim. Acta* 1983, 79:93-94.
[65] Li G, Jiang K, Zaman S, Xuan J, Wang Z, *et al*. Ti3C2 sheets with an adjustable surface and feature sizes to regulate the chemical stability. *Inorg. Chem.* 2019, 58(14):9397–9403.
[66] Li T, Yao L, Liu Q, Gu J, Luo R, *et al*. Fluorine-Free synthesis of High-Purity Ti3C2T (T=OH, O) via alkali treatment. *Angew. Chem. Int. Ed.* 2018, 57(21):6115–6119.
[67] Peng C, Wei P, Chen X, Zhang Y, Zhu F, *et al*. A hydrothermal etching route to synthesis of 2D MXene (Ti3C2, Nb2C): Enhanced exfoliation and improved adsorption performance. *Ceram. Int.* 2018, 44(15):18886–18893.
[68] Wang W, Lu M, Fang S, Li G, Wang J, *et al.* Preparation and characterization of Ti3C2 Mxene through back propagation neural network-genetic algorithm combined with surface method response. *Process Saf. Environ. Prot.* 2024, 190:316–325.
[69] Zhao M, Wu E, Li D, Luo J, Zhang X, *et al*. Development of a baseline model for MAX/MXene synthesis recipes extraction via pre-trained model with domain knowledge. *J. Mater. Res. Technol.* 2023, 22:2262–2274.
[70] Arole K, Blivin JW, Saha S, Holta DE, Zhao X, *et al*. Water-dispersible Ti3C2Tz MXene nanosheets by molten salt etching. *iScience* 2021, 24(12):103403.
[71] Yao Y, Wang Z, Wang W, Han Y, Zhu Z. High-intensity ultrasonic exfoliation-assisted rapid preparation of MXene for gas sensing. *Chem. Eng. J.* 2024, 489:151140.
[72] Karahan HE, Goh K, Zhang C, Yang E, Yıldırım C, *et al.* MXene materials for designing advanced separation membranes. *Adv. Mater.* 2020, 32(29):1906697.
[73] Zhang L, Wei K, Zeng G, Lin Q, Liu X, *et al*. High-efficient oil/water separation membrane based on MXene nanosheets by co-incorporation of APTES and amine functionalized carbon nanotubes. *J. Environ. Chem. Eng.* 2021, 9(6):106658.
[74] Mu X, Chen L, Qu N, Yin M, Wu S, *et al.* MXene/Ag3PO4 modified PVDF composite membranes for efficient interfacial evaporation and photodegradation. *J. Environ. Chem. Eng.* 2024, 12(3):112869.
[75] Liu J, Zhang H-B, Sun R, Liu Y, Liu Z, *et al.* Hydrophobic, flexible, and lightweight mxene foams for high-performance electromagnetic-interference shielding. *Adv. Mater.* 2017, 29(38):1702367.
[76] Han R, Xie Y, Ma X. Crosslinked P84 copolyimide/MXene mixed matrix membrane with excellent solvent resistance and permselectivity. *Chin. J. Chem. Eng.* 2019, 27(4):877–883.
[77] Zhi W, Xiang S, Bian R, Lin R, Wu K, *et al*. Study of MXene-filled polyurethane nanocomposites prepared via an emulsion method. *Compos. Sci. Technol.* 2018, 168:404–411.
[78] Altinkaya SA, Ozbas B. Modeling of asymmetric membrane formation by dry-casting method. *J. Membr. Sci.* 2004, 230(1):71–89.
[79] Li M, Zhang P, Wang Q, Yu N, Zhang X, *et al*. Electrospinning novel sodium alginate/MXene nanofiber membranes for effective adsorption of methylene blue. *Polymers* 2023, 15(9):2110.
[80] Cheng H, Yang C, Chu J, Zhou H, Wang C. Multifunctional Ti3C2Tx MXene/nanospheres/Ti3C2Tx MXene/thermoplastic polyurethane electrospinning membrane inspired by bean pod structure for EMI shielding and pressure sensing. *Sens. Actuators, A* 2023, 353:114226.

[81] Hu Y, Chen Z, Ding Y, Xu Y, Lin H, *et al*. Nanofiltration membranes fabricated by plant polyphenol-intermediated MXene and polyethyleneimine layer-by-layer self-assembly for efficient dye/salt separation. *Sep. Purif. Technol.* 2023, 323:124343.
[82] Purbayanto MAK, Bury D, Chandel M, Shahrak ZD, Mochalin VN, *et al*. Ambient processed rGO/Ti3CNTx MXene thin film with high oxidation stability, photosensitivity, and self-cleaning potential. *ACS Appl. Mater. Interfaces* 2023, 15(37):44075–44086.
[83] Purbayanto MAK, Chandel M, Bury D, Wójcik A, Moszczyńska D, *et al*. Microwave-assisted hydrothermal synthesis of photocatalytic truncated-bipyramidal TiO(2)/Ti(3)CN heterostructures derived from Ti(3)CN MXene. *Langmuir* 2024, 40(41):21547–21558.
[84] Zhang H, Wang L, Chen Q, Li P, Zhou A, *et al*. Preparation, mechanical and anti-friction performance of MXene/polymer composites. *Mater. Des.* 2016, 92:682–689.
[85] Santos DMF, Sequeira CAC, Figueiredo JL. Hydrogen production by alkaline water electrolysis. *Quim. Nova* 2013, 36:1176–1193.
[86] Chen C, Tse Y-LS, Lindberg GE, Knight C, Voth GA. Hydroxide solvation and transport in anion exchange membranes. *J. Am. Chem. Soc.* 2016, 138(3):991–1000.
[87] Li Z, He X, Jiang Z, Yin Y, Zhang B, *et al*. Enhancing hydroxide conductivity and stability of anion exchange membrane by blending quaternary ammonium functionalized polymers. *Electrochim. Acta* 2017, 240:486–494.
[88] Agmon N. The Grotthuss mechanism. *Chem. Phys. Lett.* 1995, 244(5):456–462.
[89] Li N, Yan T, Li Z, Thurn-Albrecht T, Binder WH. Comb-shaped polymers to enhance hydroxide transport in anion exchange membranes. *Energy Environ. Sci.* 2012, 5(7):7888–7892.
[90] Dean JA. Lang's handbook of chemistry. *Mater. Manuf. Processes* 1990, 5(4): 687–688.
[91] P V. Ionic conductivity and diffusion at infinite dilution. In *CRC Handbook of Chemistry and Physics*, 92nd ed. London: Taylor & Francis Online, 2011, pp. 3.
[92] Milner ST. Chain architecture and asymmetry in copolymer microphases. *Macromolecules* 1994, 27:2333–2335.
[93] Tsang EM, Zhang Z, Shi Z, Soboleva T, Holdcroft S. Considerations of macromolecular structure in the design of proton conducting polymer membranes: graft versus diblock polyelectrolytes. *J. Am. Chem. Soc.* 2007, 129(49):15106–15107.
[94] Zhang Z, Chalkova E, Fedkin M, Wang C, Lvov SN, *et al*. Synthesis and characterization of poly(vinylidene fluoride)-g-Sulfonated polystyrene graft copolymers for proton exchange membrane. In *Fuel Cell Chemistry and Operation*, American Chemical Society, 2010, pp. 31–48.
[95] Hatakeyama K, Hirose K, Awaya K, Koinuma M, Kameda N, *et al.* The effect of layer distance and oxygen content for tuning ion permeation through graphene oxide membrane. *Chem. Lett.* 2017, 47(3):292–295.
[96] Ren CE, Hatzell KB, Alhabeb M, Ling Z, Mahmoud KA, *et al*. Charge- and Size-Selective Ion sieving through Ti3C2Tx MXene membranes. *J. Phys. Chem. Lett.* 2015, 6(20):4026–4031.
[97] Wu Y, Ding L, Lu Z, Deng J, Wei Y. Two-dimensional MXene membrane for ethanol dehydration. *J. Membr. Sci.* 2019, 590:117300.
[98] Lipatov A, Alhabeb M, Lukatskaya MR, Boson A, Gogotsi Y, *et al.* Effect of synthesis on quality, electronic properties and environmental stability of individual monolayer Ti3C2 MXene flakes. *Adv. Electron. Mater.* 2016, 2(12):1600255.
[99] Ding M, Xu H, Chen W, Yang G, Kong Q, *et al*. 2D laminar maleic acid-crosslinked MXene membrane with tunable nanochannels for efficient and stable pervaporation desalination. *J. Membr. Sci.* 2020, 600:117871.
[100] Berdiyorov GR, Mahmoud KA. Effect of surface termination on ion intercalation selectivity of bilayer Ti3C2T2 (T=F, O and OH) MXene. *Appl. Surf. Sci.* 2017, 416:725–730.
[101] Ibragimova R, Erhart P, Rinke P, Komsa HP. Surface functionalization of 2D MXenes: Trends in distribution, composition, and electronic properties. *J. Phys. Chem. Lett.* 2021, 12(9):2377–2384.
[102] Du Y, Yan Z, You W, Men Q, Chen G, *et al*. Balancing mxene surface termination and interlayer spacing enables superior microwave absorption. *Adv. Funct. Mater.* 2023, 33(34):2301449.
[103] Dahlqvist M, Rosen J. Chalcogen and halogen surface termination coverage in MXenes—

structure, stability, and properties. *npj 2D Mater. Appl.* 2024, 8(1):65.
[104] Wang X, Li H, Li H, Lin S, Ding W, *et al*. 2D/2D 1T-MoS2/Ti3C2 MXene heterostructure with excellent supercapacitor performance. *Adv. Funct. Mater.* 2020, 30(15):0190302.
[105] Li J, Yuan X, Lin C, Yang Y, Xu L, et al. Achieving high pseudocapacitance of 2d titanium carbide (MXene) by cation intercalation and surface modification. *Adv. Energy Mater* 2017, 7(15):1602725.
[106] Zheng S, Zhang C, Zhou F, Dong Y, Shi X, *et al.* Ionic liquid pre-intercalated MXene films for ionogel-based flexible micro-supercapacitors with high volumetric energy density. *J. Mater. Chem. A* 2019, 7(16):9478–9485.
[107] Fan Y, Wei L, Meng X, Zhang W, Yang N, *et al.* An unprecedented high-temperature-tolerance 2D laminar MXene membrane for ultrafast hydrogen sieving. *J. Membr. Sci.* 2019, 569:117–123.
[108] Xing C, Liu L, Guo X, Zhang M, Zhou M, *et al*. Efficient water purification using stabilized MXene nanofiltration membrane with controlled interlayer spacings. *Sep. Purif. Technol.* 2023, 317:123774.
[109] Pandey RP, Rasheed PA, Gomez T, Azam RS, Mahmoud KA. A fouling-resistant mixed-matrix nanofiltration membrane based on covalently cross-linked Ti3C2TX (MXene)/cellulose acetate. *J. Membr. Sci.* 2020, 607:118139.
[110] Shen L, Pei X, Han J, Zhang T, Li P, *et al*. Eco-friendly construction of dye-fouled loose CS/PAN nanofibrous composite membranes for permeability-selectivity anti-trade-off property. *Colloids Surf., A* 2019, 569:145–155.
[111] Wan S, Li X, Wang Y, Chen Y, Xie X, *et al*. Strong sequentially bridged MXene sheets. *PNAS* 2020, 117(44):27154–27161.
[112] Luo S, Xiang T, Dong J, Su F, Ji Y, *et al*. A double crosslinking MXene/cellulose nanofiber layered film for improving mechanical properties and stable electromagnetic interference shielding performance. *J. Mater. Sci. Technol.* 2022, 129:127–134.
[113] Wan S, Li X, Chen Y, Liu N, Du Y, *et al*. High-strength scalable MXene films through bridging-induced densification. *Science* 2021, 374(6563):96–99.
[114] Zhang L, Zhao Y, Deng Z, Liu X, Chen Y, *et al*. Preparation of sepiolite modified MXene composite membrane for oil/water separation. *J. Appl. Polym. Sci.* 2022, 139(29):e52658.
[115] Yan J, Ren CE, Maleski K, Hatter CB, Anasori B, *et al*. Flexible MXene/Graphene films for ultrafast supercapacitors with outstanding volumetric capacitance. *Adv. Funct. Mater.* 2017, 27(30):1701264.
[116] Halim J, Kota S, Lukatskaya MR, Naguib M, Zhao M, *et al*. Synthesis and characterization of 2D molybdenum carbide (MXene). *Adv. Funct. Mater.* 2016, 26(18):3118–3127.
[117] Ling Z, Ren CE, Zhao MQ, Yang J, Giammarco JM, *et al*. Flexible and conductive MXene films and nanocomposites with high capacitance. *Proc. Natl. Acad. Sci. U. S. A.* 2014, 111(47):16676–16681.
[118] Yang X, Wang Q, Zhu K, Ye K, Wang G, *et al*. 3D porous Oxidation-Resistant MXene/Graphene architectures induced by *in situ* zinc template toward High-Performance supercapacitors. *Adv. Funct. Mater.* 2021, 31(20):2101087.
[119] Sun C, Zuo P, Sun W, Xia R, Dong Z, *et al.* Self-assembly of alternating stacked 2D/2D Ti3C2Tx MXene/ZnMnNi LDH van der waals heterostructures with ultrahigh supercapacitive performance. *ACS Appl. Energy Mater.* 2020, 3(10):10242–10254.
[120] Ajibade TF, Tian H, Hassan Lasisi K, Xue Q, Yao W, et al. Multifunctional PAN UF membrane modified with 3D-MXene/O-MWCNT nanostructures for the removal of complex oil and dyes from industrial wastewater. *Sep. Purif. Technol.* 2021, 275:119135.
[121] Gong X, Zhang G, Dong H, Wang H, Nie J, et al. Self-assembled hierarchical heterogeneous MXene/COF membranes for efficient dye separations. *J. Membr. Sci.* 2022, 657:120667.
[122] Zu W, Jiang C, Liu W, Hou Q, Ji X. Fabrication of a Carbonized Cellulose Nanofibrils/Ti3C2Tx MXene/g-C3N4 Heterojunction for Visible-Light-Driven Photocatalysis. *Langmuir* 2022, 38(43):13109–13120.
[123] Shariq M, Marimuthu S, Dixit AR, Chattopadhyaya S, Pandiaraj S, *et al*. Machine learning models for prediction of electrochemical properties in supercapacitor electrodes using MXene

and graphene nanoplatelets. *Chem. Eng. J.* 2024, 484:149502.
[124] Guo W, Ma Z, Chen Z, Hua H, Wang D, *et al.* Thin and soft Ti3C2Tx MXene sponge structure for highly sensitive pressure sensor assisted by deep learning. *Chem. Eng. J.* 2024, 485:149659.
[125] Shrestha S, Barvenik KJ, Chen T, Yang H, Li Y, *et al*. Machine intelligence accelerated design of conductive MXene aerogels with programmable properties. *Nat. Commun.* 2024, 15(1):4685.
[126] Mullani NB, Kumbhar DD, Lee D-H, Kwon MJ, Cho S-y, *et al.* Surface modification of a titanium carbide MXene memristor to enhance memory window and low-power operation. *Adv. Funct. Mater.* 2023, 33(26):2300343.
[127] Yao H, Wu R, Zou J, Liu J, Peng G, *et al.* A machine learning strategy-incorporated BiFeO3/Ti3C2 MXene electrochemical platform for simple, rapid detection of Pb2+ with high sensitivity. *Chemosphere* 2023, 340:139728.
[128] Bhardwaj R, Hazra A. MXene-based gas sensors. *J. Mater. Chem. C* 2021, 9(44):15735-15754.
[129] Li Q, Li Y, Zeng W. Preparation and application of 2D MXene-Based gas sensors: A review. *Chemosensors* 2021, 9(8):225.
[130] Ma C, Ma M, Si C, Ji X, Wan P. Flexible MXene-Based composites for wearable devices. *Adv. Funct. Mater.* 2021, 31(22):2009524.
[131] Sreenilayam SP, Ul Ahad I, Nicolosi V, Brabazon D. MXene materials based printed flexible devices for healthcare, biomedical and energy storage applications. *Mater. Today* 2021, 43:99–131.
[132] Pitcheri R, Chittibabu SK, Sangaraju S, Jarsangi B, Al-Asbahi BA, *et al*. Emerging trends of 3D architectonic MXene-based flexible pressure sensors as multimodal medical devices. *Coord. Chem. Rev.* 2024, 499:215527.
[133] Lyu B, Choi Y, Jing H, Qian C, Kang H, *et al.* 2D MXene-TiO2 Core-Shell nanosheets as a Data-Storage medium in memory devices. *Adv. Mater.* 2020, 32(17):1907633.
[134] Tahir R, Fatima S, Zahra SA, Akinwande D, Li H, *et al*. Multiferroic and ferroelectric phases revealed in 2D Ti3C2Tx MXene film for high performance resistive data storage devices. *npj 2D Mater. Appl.* 2023, 7(1):7.
[135] Liu X, Chen D, Yang C, Li Y, Feng Y, *et al.* Study on energy and information storage properities of 2D-MXene/polyimide composites. *Composites, Part B* 2022, 241:110014.
[136] Jamil F, Ali HM, Janjua MM. MXene based advanced materials for thermal energy storage: A recent review. *J. Energy Storage* 2021, 35:102322.
[137] Cao J, Zhou Z, Song Q, Chen K, Su G, *et al*. Ultrarobust Ti3C2Tx MXene-Based soft actuators via bamboo-inspired mesoscale assembly of hybrid nanostructures. *ACS Nano* 2020, 14(6):7055–7065.
[138] Umrao S, Tabassian R, Kim J, Nguyen VH, Zhou Q, *et al*. MXene artificial muscles based on ionically cross-linked $Ti_3C_2T_x$ electrode for kinetic soft robotics. *Sci. Rob.* 2019, 4(33):eaaw7797.
[139] Iravani S, Khosravi A, Nazarzadeh Zare E, Varma RS, Zarrabi A, *et al*. MXenes and artificial intelligence: fostering advancements in synthesis techniques and breakthroughs in applications. *RSC Adv.* 2024, 14(49):36835–36851.
[140] Shahzad F, Iqbal A, Kim H, Koo CM. 2D transition metal carbides (MXenes): Applications as an electrically conducting material. *Adv. Mater.* 2020, 32(51):2002159.
[141] Shuck CE, Sarycheva A, Anayee M, Levitt A, Zhu Y, *et al*. Scalable Synthesis of Ti3C2T MXene. *Adv. Eng. Mater.* 2020, 22(3):1901241.
[142] Purbayanto MAK, Presser V, Skarżyński K, Słoma M, Naguib M, *et al*. MXenes: Multifunctional materials for the smart cities of tomorrow. *Adv. Funct. Mater.* 2024, 2409953.
[143] Chaudhary V, Kaushik A, Furukawa H, Khosla A. Review—Towards 5th generation AI and IoT driven sustainable intelligent sensors based on 2D MXenes and borophene. *ECS Sens. Plus* 2022, 1(1):013601.